NONLINEAR DYNAMIC PHENOMENA IN CIRCUITS

When we look at the behavior of the state in a nonlinear circuit, its long-term time response is sometimes remarkably different from that of a linear circuit. In some cases we come across phenomena that never occur in linear circuits. These are termed *nonlinear phenomena.* The existence of multistable states, self-excited oscillation, nonlinear resonances, synchronizations, and chaotic states, all of which occur naturally in simple nonlinear circuits, illustrate typically these particular phenomena. In a linear circuit or system, there exists only one steady state and all transient states die out after appropriately long time duration. Linear systems have a nice property such that we can always analyze the steady and transient states separately by the principle of superposition. Hence we know all the properties of linear systems by analytical treatment. In nonlinear systems, on the other hand, besides the local property of linear systems there may appear some combined or mixed states that have qualitatively different features, and this fact causes some complicated behavior of states in time. Because there is no general analytical solution for these nonlinear phenomena, the problem is difficult. Much attention has been paid to the problem, however, in the last two decades, and the progress of theoretical and applied study in the field of nonlinear dynamics has developed rapidly.

Apart from the circuit dynamics, these nonlinear phenomena are very commonly observed in many other disciplines, such as mechanics, physical systems, chemical reactions, optics, fluid dynamics, and population dynamics. The mathematical model of these systems is expressed by a system of ordinary differential equations which defines a deterministic process, called a *dynamical system.* The theory of dynamical systems is then concerned primarily with making qualitative investigations into the behavior of states which evolve in time, as the initial state and parameter of the system are varied. Most of the models derived from practical problems cannot be solved by analytic method, so that the topological or geometrical approach (called the *qualitative method*) and numerical analyses are of fundamental importance in understanding of various phenomena observed in dynamical systems. Fortunately, among many nonlinear systems, electrical circuits are considered simple and convenient physical systems to implement real nonlinear phenomena. They are themselves widely used in various fields of electrical engineering.

Dynamical Process, State, State Space, and Attractor

Now we proceed with a little more detailed overview of some typical nonlinear phenomena, some of which will also be discussed in later sections. Mathematically, the dynamic process of a circuit is formulated as a set of ordinary differential equations, where the time is the independent variable and states of the circuit are dependent variables in time. The equations, say circuit dynamics, give a law of the evolution of the state and determine the time evolution of all states of the circuit. All possible states are then characterized by the points of some point set or space, called a *state space.* The state space is also called a *phase space,* borrowing from classical mechanics. Actually, the specification of a point in the state space is sufficient to describe the initial or current state, as well as to determine its future evolution. Then, for a given initial point in the state space, the state evolves by the circuit dynamics. One of the salient features of circuit dynamics is its dissipative property, which is achieved by resistors. Usually a circuit consists of energy-storing elements (i.e., inductors and capacitors) and energy dissipative elements (i.e., resistors). Hence along the time evolution of state the energy stored in the circuit will be lost at resistors and its state will approach some stable steady state in the state space. The steady state works as if it absorbs every neighboring state into itself. Such a steady state is called an *attractor,* and the existence of attractors is the most significant property of a dissipative system such as the circuit dynamics. On the other hand, a lossless circuit containing only inductors and capacitors is formulated as an energy conservative system similar to classical mechanics. In this case we have no attractors and the distinction between transient state and steady state becomes difficult.

Examples of Steady State and Attractor

Among all possible states in the state space, some particular states have a special property such that they are invariant in some sense during the time evolution. They are candidates to be attractors or steady states of the system. Equilibrium point, periodic state, quasiperiodic state, and a more complicated state, called *chaotic state,* are typical invariant sets of the system. An equilibrium point, also called a *rest point,* is a single point in the state space which always rests at the same point during the time evolution. This is the simplest steady state and corresponds to a dc operating point in a real circuit. Periodic state is a periodically repeated state with a definite period or frequency. This state is commonly observed in forced circuits driven by an ac voltage or current source. An oscillator also produces a periodic state. Many biological rhythms are also modeled as periodic states generated by biological oscillators. A state containing several distinct frequencies is called a *quasiperiodic state.* It appears sometimes in a forced oscillator with periodic input signal. When the difference of free and driving frequencies is appropriately large, both frequencies can survive and doubly periodic oscillation becomes possible. In this case the time response is a beat or quasi-periodic oscillation. Chaotic state is the most complicated state whose long-term time response looks like a noisy or random nature. Later we will discuss this state more precisely. The concept of stability of the above invariant sets is also important. Roughly speaking, a steady state is stable if every neighboring state always stays in the neighborhood of the steady state in future evolution. If a steady state satisfies a stronger condition such that all neighbors approach the steady state, then we say that the state is asymptotically stable. An attractor is an asymptotically stable steady state. In a real system a physically observable state is an attractor. In the theory of dynamical systems the above invariant sets are called *nonwandering sets.* On the other hand, a transient state corresponds to a wandering set. Figure 1 shows schematic diagram of states of dynamical systems and their bifurcations.

Role of System Parameters

A steady state of a circuit depends also on parameters contained in circuit dynamics. Associated with the change of parameters, the qualitative property of a steady state may change at some particular value of the parameters. For example, the appearance of a couple of steady states, stability change of a steady state, or the creation of a new type of steady state, and so on, may occur under the variation of parameters. We may imagine the parameters as a controlling device of the qualitative property of states. That is, by changing system parameters we can see a morphological process of steady states, which is referred to as a *bifurcation of state* or

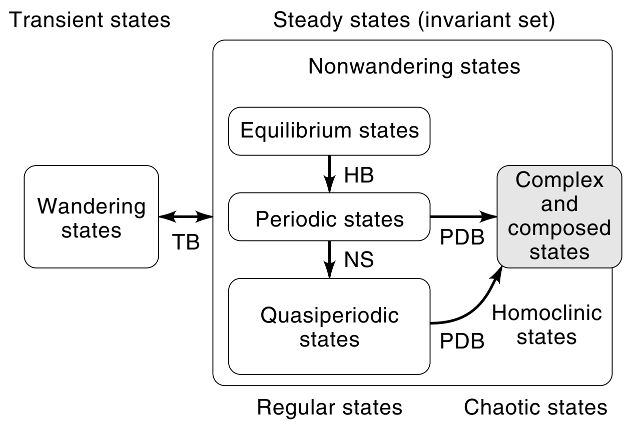

Figure 1. Schematic diagram of states of dynamical systems and their bifurcations. TB, HB, NS, and PDB indicate tangent bifurcation, Hopf bifurcation, Neimark–Sacker bifurcation, and period doubling bifurcation, respectively.

a *bifurcation phenomenon.* Bifurcations indicated by arrows in Fig. 1 will be discussed in later sections.

Typical Nonlinear Phenomena

In the following we will present a short review of typical nonlinear phenomena. More concrete examples will be given in subsequent sections. Figure 2 shows a schematic diagram of nonlinear phenomena and related bifurcations.

Multistable States. Several stable steady states can coexist in nonlinear systems. The simplest example is a flip-flop action with two stable equilibrium points as attractors. Depending on a given initial state, the state starts to evolve and falls into one of the attractors. Which attractor is finally realized is uniquely determined by the choice of the initial state.

Self-Excited Oscillation. An *LC* resonant circuit with a negative resistance is a simple sinusoidal oscillator which generates a stable periodic state in two-dimensional state space, called a *phase plane.* The circuit has only a dc source and no periodic inputs or periodic forces. But a dc operating point (i.e., an equilibrium point) becomes unstable because of the negative resistance and a periodic state appears. The oscillatory state is then represented as a closed curve in the phase plane and is called a *limit cycle.* A small initial state grows up and approaches the closed curve, whereas a large initial state shrinks asymptotically into the same closed curve. Hence the limit cycle is a unique attractor of the circuit. This is a simplest mechanism of self-excited oscillatory process. A sinusoidal time response is obtained for a weak nonlinear system, called a *nearly harmonic oscillator.* On the other hand, if the nonlinear characteristics is strong, we may observe a nearly square wave response, called a *relaxation oscillation.*

Nonlinear Resonance. This phenomenon occurs mainly in a nonlinear resonant circuit driven by a periodic input signal. A ferro-resonant circuit forced by an ac voltage source is a typical example of this type of circuit. As the system is forced by a periodic external input signal, the steady state may be realized by a periodic, quasiperiodic, or chaotic state. For a moment we consider only the case where the steady state oscillates with the same frequency as that of the injected periodic signal. Keeping the amplitude of the forcing function constant and also changing the frequency of the input signal, we observe a range of frequencies for which several possible stable periodic states coexist. Under the gradual change of frequency a hysteretic effect between the stable steady states occurs for increasing and decreasing frequencies. This is called a *jump phenomenon of nonlinear resonance.* Other periodic states can be also observed such as subharmonic or higher-harmonic oscillations, whose frequency is a fraction or an integral multiple of that of the input signal, respectively. Therefore by nonlinear resonances there may appear multistable states of periodic oscillations with various frequencies. Bifurcations of steady states occur by changing external injected frequency. The same phenomenon is also observed by changing the amplitude of the external signal whereas the frequency is held constant. Note also that a driven nonlinear resonant circuit exhibits many other phenomena, such as the period doubling bifurcation, the appearance of quasiperiodic states, chaotic states, and so on.

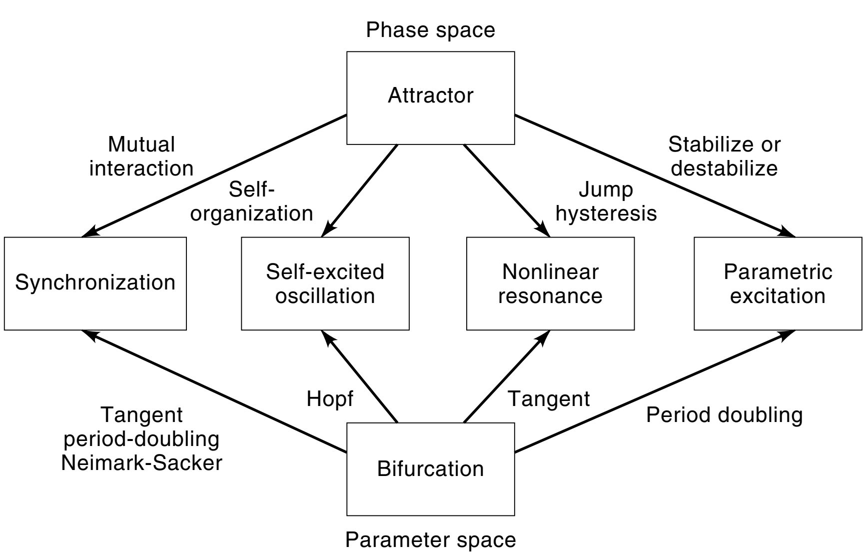

Figure 2. Schematic diagram of typical nonlinear phenomena: synchronization, self-excited oscillation, nonlinear resonance, and parametric excitation.

Period Doubling Bifurcation. In a periodically driven circuit we may observe that a stable periodic state becomes unstable and there appears another stable periodic state with half-frequency under the variation of system parameters. That is, the new periodic state has a period that is exactly twice as long. This is a period doubling bifurcation and is one of the general bifurcation processes of the periodic state. In many cases under the finite change of parameters, this doubling process repeats successively infinitely many times. At every doubling process a new periodic state with half-frequency is produced. Hence after this cascade of period doubling bifurcations we observe a strange and complicated oscillatory state possibly with very low frequencies, called a *chaotic state.* The cascade is thus considered one of the routes to produce a chaotic state.

Chaotic State. A chaotic state is a set of bounded composite steady states composed of infinitely many unstable periodic and nonperiodic states. Hence the long time response of the state looks like a noisy or random oscillation. In a chaotic attractor every state is unstable in one direction and stable in another direction so that the neighboring states diverge at some instant and converge at another instant during the time evolution. All states in the attractor are thus mixing each other according to the nonlinear property of the dynamics. Thus two states starting from slightly different initial states diverge rapidly so that the initial information of states will be violated. This property is referred to as a *sensitive dependence of intial states.* A chaotic state is commonly observed after a cascade of period doubling bifurcation stated above. Because we cannot explicitly solve the circuit dynamics, the complexity of the attractor is still mathematically unsolved. We can see, however, some qualitative properties by topological and/or numerical approaches.

Synchronization. A synchronization effect can readily be realized by a sinusoidal oscillator driven by an external sinusoidal signal. When the frequency difference of the free oscillator and driving input signal is appropriately large, quasiperiodic states appear. At a certain difference of the frequencies the quasiperiodic states suddenly disappear and there remains an entrained periodic state with single external frequency. Similar entrainment can occur when we couple two or more oscillators with nearly equal frequencies. The former is called a *frequency entrainment* or *phase locked phenomenon,* whereas the latter is called a *mutual synchronization.* Human circadian rhythms being entrained by the earth rotation clock is a former example. For the latter example, we see that despite many power stations being connected, a power network operates at a single frequency.

Parametric Excitation. Parametric excitation or parametric resonance is an oscillatory phenomenon observed in a system with periodically varying parameters. A periodic external signal is injected into a system parameter in this case. An *RLC* parallel circuit with a mechanically varying capacitance is a simple example of this type of circuit, called a *parametric amplifier.* Applying a sinusoidal signal, the pump signal, to the mechanical part, we can realize a periodically varying capacitance. In this circuit under appropriate setting of parameters there appears a period doubling bifurcation of state; that is, a stable equilibrium point becomes unstable and there appears a periodic state with half-frequency of the external mechanical input. The vertically pumping of a swing by a child is another example of a parametrically excited system. In an oscillatory regime the horizontal frequency is approximately half that of the body of the child.

Method of Analysis

For understanding dynamical processes we have to know many mathematical objects: the geometry of phase portrait, approximation methods of periodic states, time series analysis for chaotic responses, mechanism of bifurcation process, and so on (see Fig. 3). Various methods of analyses have been proposed to this end. Here we point out briefly three different approaches as follows.

Analytical Method. The method of analyzing periodic states is well developed for weakly nonlinear systems. Various perturbation methods and averaging methods are classically applied to determine the periodic states of free and forced electrical circuits. For systems with strong nonlinearity, little is known. Galerkin's method of combining numerical analysis is one of the methods for obtaining periodic states for such strong nonlinear systems. Probability theory or ergodic theory will be applied to the analysis of chaotic state in order to know the long-term behavior.

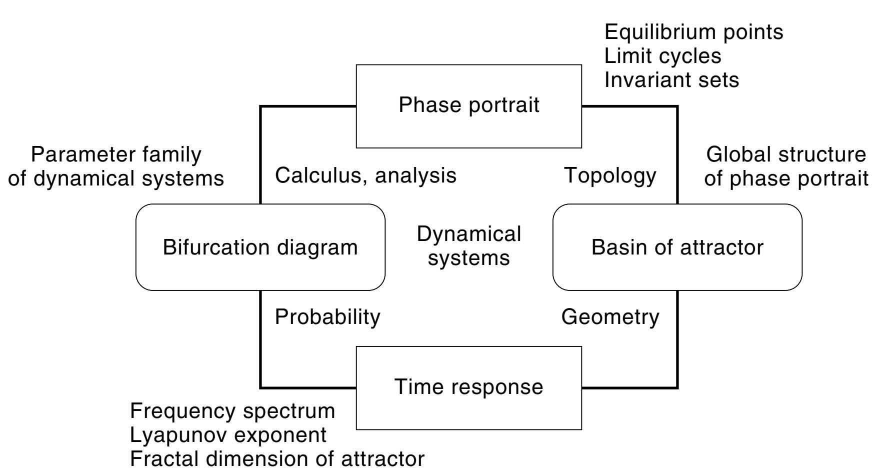

Figure 3. Schematic diagram of the analysis of dynamical systems.

Geometrical or Topological Method. Although nonlinear ordinary differential equations cannot generally be solved explicitly by quadrature, we can know the existence of a solution with a given initial condition, the uniqueness property of the solution, extendability of the solution in long time interval, asymptotic property of solution, stability of the solution, and so on. These properties depend upon the geometrical or mainly topological property of dynamical systems. A qualitative approach is then directed to the study of phase portraits, stability theory, and bifurcation processes.

Numerical Method or Simulation. Many numerical integration methods are now available. Combining these integration methods and the qualitative approach, we can calculate any type of steady state, stability condition, bifurcation condition, statistical test condition for chaotic states, and so on. Newton's method and other root finding methods are effectively used for the numerical computations.

References in This Section

The theory of dynamical systems, especially classical mechanics, has a long history and has developed many useful techniques to study the time evolution of state. During the early part of the twentieth century, the theory of nonlinear oscillations arose in electrical and mechanical engineering and has been developed also in parallel with that of dynamical systems. After discovering the chaotic state in many applied fields, the nonlinear dynamics has become popular during the last two decades. Many books and references are now available. We refer to only classical books (1–9) about nonlinear oscillations in circuit dynamics and dynamical systems.

BASIC MATHEMATICAL FACTS

In this section we review minimal mathematical tools for understanding the circuit dynamics as a time-evolving process called a *dynamical system.* We also mainly treat a smooth system; that is, the functions or maps defining the system will be differentiable as many times as we want. In the remainder of the article the term *dynamical system* refers to a differentiable dynamical system or simply a smooth dynamical system.

Circuit Dynamics, State and State Equation

Every lumped electrical circuit obeys two basic physical laws: (1) Kirchhoff's voltage and current laws and (2) the element characteristics derived from the constitutive relation of circuit element. Combining these two constraint relations and eliminating auxiliary variables, we can obtain a system of first-order ordinary differential equations in normal form as the state equation or circuit dynamics of the circuit:

$$\dot{\mathbf{x}} = \mathbf{f}(t, \mathbf{x}, \lambda) \tag{1}$$

where t is the time: $t \in \mathbf{R}$,

$$\mathbf{x} = \begin{bmatrix} x_1 \\ x_2 \\ \vdots \\ x_n \end{bmatrix} \in \mathbf{R}^n, \qquad \lambda = \begin{bmatrix} \lambda_1 \\ \lambda_2 \\ \vdots \\ \lambda_m \end{bmatrix} \in \mathbf{R}^m$$

are the state vector and the system parameter, respectively, and the dot over $\mathbf{x}$ denotes differentiation with respect to the time: $\dot{\mathbf{x}} = d\mathbf{x}/dt$. In most cases the voltages across capacitors (or charges stored in capacitors) and the currents through inductors (or magnetic flux linkages in inductors) will constitute the set of state variables $x_1, x_2, \ldots, x_n$. The state $\mathbf{x}$ is then considered as a point of n-dimensional Euclidean space: $\mathbf{x} \in \mathbf{R}^n$, where n is the sum of the number of capacitors and inductors in the circuit. The function $\mathbf{f}$ of the right-hand side of Eq. (1) gives the velocity vector at each point in the state space and determines the dynamics of the circuit. That is, Eq. (1) defines a vector field in the state space. If $\mathbf{f}$ does not contain the time explicitly, then Eq. (1) is called *autonomous.* Otherwise, Eq. (1) is called *nonautonomous.* An autonomous equation defines a time-invariant vector field in the state space $\mathbf{R}^n$, whereas a nonautonomous equation defines a time varying vector field in $\mathbf{R}^n$. In circuit dynamics an autonomous system arises mainly from a circuit containing only dc sources. A typical example of a nonautonomous system is a circuit driven by an ac source.

Remark 1. 1. In the above definition we assume that the state space of Eq. (1) is an entire n-dimensional Euclidean space $\mathbf{R}^n$. In some cases it may happen that the vector field (1) is defined only some bounded region or some subset of $\mathbf{R}^n$. The same situation occurs for other variables: time and parameters. For convenience we assume that the state space is simply the whole $\mathbf{R}^n$. In our circuit application, however, we interest the time evolution of the state within the bounded region.

2. The function $\mathbf{f}$ in Eq. (1) reveals the element characteristics and the connection of the circuit elements. Hence, if the element characteristics are defined by continuous or differentiable functions, then $\mathbf{f}$ becomes continuous or differentiable functions, respectively. If the characteristics is assumed as a piecewise linear function, then $\mathbf{f}$ is expressed by a piecewise linear function. In the following we will mainly consider the case where $\mathbf{f}$ is defined everywhere and differentiable with all variables t, $\mathbf{x}$ and λ.

3. For the nonlinear circuit with weakly nonlinear characteristics, Eq. (1) may be expressed by the form

$$\dot{\mathbf{x}} = \mathbf{A}\mathbf{x} + \mathbf{g}(t) + \epsilon\mathbf{f}(t, \mathbf{x}) \tag{2}$$

where $\mathbf{A}$ is an $n \times n$ constant matrix and ϵ is a small parameter of real number. In this case we say Eq. (2) a quasilinear system or a weakly nonlinear system.

Example 1. 1. An *RLC* resonant circuit. Consider the *RLC* resonant circuit with a negative conductor shown in Fig. 4(a).

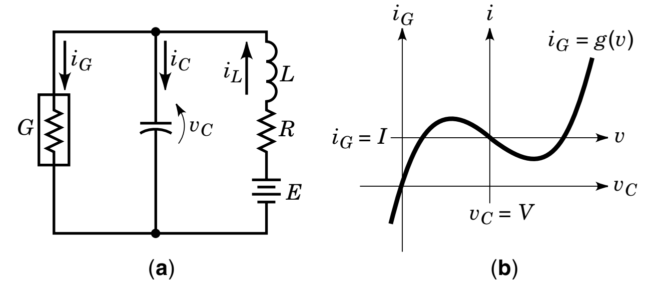

Figure 4. (a) *RLC* resonant oscillator and (b) characteristics of the nonlinear conductor.

We assume that the capacitor and inductor have linear characteristics whereas the conductor G has a nonlinear characteristics with voltage controlled type [see Fig. 4(b)]. For convenience we assume the nonlinear characteristics as a cubic polynomial. Then the constitutive relations are written as

$$\begin{aligned} i_C &= C\frac{dv_C}{dt}, \\ v_L &= L\frac{di_L}{dt}, \\ i_G &= g(v_G) = I_G - G_1 v_G - G_2 v_G^2 + G_3 v_G^3; \\ & G_1, G_2, G_3 > 0 \end{aligned} \tag{3}$$

By choosing the capacitor's voltage and the inductor's current as the state variables we have the state equations:

$$\begin{aligned} C\frac{dv_C}{dt} &= i_L - i_G = i_L - g(v_C) \\ L\frac{di_L}{dt} &= -v_C - Ri_L + E \end{aligned} \tag{4}$$

If we put the system in vector normal form, we have Eq. (1) with

$$\mathbf{x} = \begin{bmatrix} v_C \\ i_L \end{bmatrix}, \qquad \mathbf{f} = \begin{bmatrix} \frac{1}{C} i_L - \frac{1}{C} g(v_C) \\ -\frac{1}{L} v_C - \frac{R}{L} i_L + \frac{E}{L} \end{bmatrix} \tag{5}$$

This gives an autonomous vector field in two-dimensional state space (v_C, i_L).

By using the coordinate translation

$$v_C = v + V, \qquad i_L = i + I, \qquad i_G = i_g + I \tag{6}$$

Eq. (4) becomes more compact form:

$$\begin{aligned} C\frac{dv}{dt} &= i + g_1 v - g_3 v^3 \\ L\frac{di}{dt} &= -v - Ri + e \end{aligned} \tag{7}$$

where we put

$$g_1 = G_1 + 2G_2 V - 3G_3 V^2, \qquad g_3 = G_3, \qquad e = V - RI + E \tag{8}$$

and V and I are determined by the following relation:

$$G_2 - 3G_3 V = 0, \qquad I = I_G - G_1 V - G_2 V^2 + G_3 V^3 \tag{9}$$

For some purposes, it is convenient to renormalize the variables as

$$x = \sqrt{C} v, \qquad y = \sqrt{L} i, \qquad \tau = \frac{1}{\sqrt{LC}} t \tag{10}$$

Equation (7) is then rewritten as

$$\begin{aligned} \frac{dx}{d\tau} &= y + \gamma_1 x - \gamma_3 x^3 \\ \frac{dy}{d\tau} &= -x - ky + B \end{aligned} \tag{11}$$

where we put the parameters as

$$\gamma_1 = g_1 \sqrt{\frac{L}{C}}, \qquad \gamma_3 = \frac{g_3}{C}\sqrt{\frac{L}{C}}, \qquad k = R\sqrt{\frac{C}{L}}, \qquad B = e\sqrt{C} \tag{12}$$

In the case where $R = 0$ and $E = 0$ (i.e., $k = 0$ and $B = 0$), by eliminating the state y from Eq. (11) we have the following second-order equation, called the *van der Pol equation:*

$$\frac{d^2x}{d\tau^2} - \gamma_1 \left(1 - 3\frac{\gamma_3}{\gamma_1} x^2\right) \frac{dx}{d\tau} + x = 0 \tag{13}$$

Equation (13) exhibits a typical self-oscillatory process of the circuit as we shall see later. Note also that if we eliminate the variable x, then we have the *Rayleigh equation:*

$$\frac{d^2y}{d\tau^2} - \gamma_1 \left\{1 - \frac{\gamma_3}{\gamma_1}\left(\frac{dy}{d\tau}\right)^2\right\} \frac{dy}{d\tau} + y = 0 \tag{14}$$

Both Eqs. (13) and (14) are expressed by the first-order form as Eq. (11), hence they are equivalent.

2. A forced resonant circuit. Figure 5 shows another resonant circuit with a saturable nonlinear inductor driven by an alternating voltage source $E \sin \omega t$. As shown in the figure, the linear resistor R is placed in parallel with the linear capacitor C, so that the circuit is dissipative. With the notation of Fig. 5, we have

$$\begin{aligned} C\frac{dv_C}{dt} + \frac{v_C}{R} &= i_L \\ n\frac{d\phi}{dt} + v_C &= E \sin \omega t \end{aligned} \tag{15}$$

where n is the number of turns of the coil and ϕ denotes the magnetic flux of the inductor. The saturable reactor has a secondary coil which only supplies a biasing direct current. Neglecting hysteresis, we assume the nonlinear characteristics of the inductor to be

$$ni_L = f(\phi) = a_1\phi + a_2\phi^2 + a_3\phi^3 \tag{16}$$

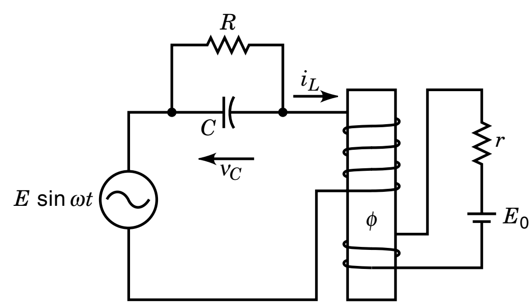

Figure 5. Forced resonant circuit with a nonlinear saturable inductor.

where a_1, a_2, and a_3 are positive constants. Substituting Eq. (16) into Eq. (15), we have the state equation:

$$\begin{aligned}\frac{dv_C}{dt} &= -\frac{v_C}{RC} + \frac{1}{nC}f(\phi)\\ \frac{d\phi}{dt} &= -\frac{1}{n}v_C + \frac{E}{n}\sin\omega t\end{aligned} \tag{17}$$

for the state variables (v_C, ϕ). This gives a nonautonomous system. By eliminating v_C, we have the following second-order equation:

$$\frac{d^2\phi}{d\tau^2} + k\frac{d\phi}{d\tau} + b_1\phi + b_2\phi^2 + b_3\phi^3 = B\cos\tau \tag{18}$$

where

$$\tau = \omega t - \tan^{-1}k, \qquad k = \frac{1}{\omega RC}, \qquad b_l = \frac{a_l}{n^2\omega^2 C}(l = 1, 2, 3),$$
$$B = \frac{E}{n\omega}\sqrt{1+k^2} \tag{19}$$

Equation (19) can be transformed to the alternative form as

$$\frac{d^2x}{d\tau^2} + k\frac{dx}{d\tau} + c_1x + c_3x^3 = B_0 + B\cos\tau \tag{20}$$

where $x = \phi + b_2/3b_3$ and c_1, c_3, B_0 are constants determined by b_1, b_2, and b_3. Equations (19) and (20) are called *Duffing's equations* and exhibit various resonant phenomena as well as jump and hysteresis of these responses.

Local Existence and Uniqueness Theorem of the Solutions of Circuit Dynamics

By returning to dynamical problems, let us consider the following initial value problem of Eq. (1). Suppose that an initial state $\mathbf{x}_0$ and an initial instant t_0 is given. We say the function

$$\mathbf{x}(t) = \varphi(t, \mathbf{x}_0, \lambda) \tag{21}$$

is a solution of Eq. (1) on a time interval $I \subset \mathbf{R}$ containing t_0, if Eq. (21) satisfies Eq. (1), that is,

$$\dot{\varphi}(t, \mathbf{x}_0) = \mathbf{f}(t, \varphi(t, \mathbf{x}_0, \lambda), \lambda) \tag{22}$$

An initial value problem for Eq. (1) consists of finding the interval I and the solution (21) satisfying the initial condition:

$$\mathbf{x}(t_0) = \varphi(t_0, \mathbf{x}_0, \lambda) = \mathbf{x}_0 \tag{23}$$

Thus we write the problem symbolically as

$$\dot{\mathbf{x}}(t) = \mathbf{f}(t, \mathbf{x}(t), \lambda), \quad \mathbf{x}(t_0) = \varphi(t_0, \mathbf{x}_0, \lambda) = \mathbf{x}_0, \qquad t \in I \subset \mathbf{R} \tag{24}$$

If such a solution exists, we refer to Eq. (21) as a solution passing through $\mathbf{x}_0$ at the instant t_0. The solution (21) is also called a trajectory starting from $\mathbf{x}_0$ at $t = t_0$. It corresponds to a time response of the state in the state space $\mathbf{R}^n$. Note that the solution is not only a function of time but also a function of the initial value as well as the system parameters. In an autonomous system the time evolution of the state is invariant under any translation of time. Hence without loss of generality we can choose the initial instance $t_0 = 0$.

Hence the questions arise. For a given initial value problem, does Eq. (1) has a solution for all $t \in I \subset \mathbf{R}$? If Eq. (1) has a solution, is such a solution unique and does it extend to the entire time interval $\mathbf{R}$? The answer is the following theorem on the local existence and uniqueness of the solution of Eq. (1).

Theorem 1. Suppose that in Eq. (1) the function $\mathbf{f}(t, \mathbf{x}, \lambda)$ is differentiable in all variables t, $\mathbf{x}$, λ, then there exists an interval $I \subset \mathbf{R}$ containing t_0 and the solution (21) also exists for all initial conditions $(t_0, \mathbf{x}_0) \in I \times \mathbf{R}^n$. Moreover, this solution is unique.

Remark 2. 1. The initial value problem (24) can be equivalently rewritten as the integral equation of the form:

$$\mathbf{x}(t) = \mathbf{x}_0 + \int_{t_0}^{t} \mathbf{f}(s, \mathbf{x}, \lambda)ds \tag{25}$$

Existence and uniqueness property is then discussed by posing an appropriate condition on $\mathbf{f}$. One of the sufficient conditions to guarantee the property is known as a *local Lipschitz condition.* Because the differentiability is stronger than the Lipschitz condition, we never worry about the existence and uniqueness problem if $\mathbf{f}$ is differentiable. Note that the solution to Eq. (21) exists only in a short time interval I so that the theorem asserts a local existence property.

2. Extendability of the solution to the entire time interval $\mathbf{R}$ depends on $\mathbf{f}(t, \mathbf{x}, \lambda)$. Usually the function $\mathbf{f}(t, \mathbf{x}, \lambda)$ is defined in a bounded region of state space $\mathbf{R}^n$. Starting with an initial state in the region, the state may reach the boundary of this region after a finite time, and the solution could no longer be extended to rest in the region. The simplest example of such behavior is a blow-up situation where a state approaches to infinity within a finite time. In most circuit applications, however, the solution can be extended to the entire time interval $\mathbf{R}$.

3. In circuit dynamics, under some particular connection of elements, the normal form of the state equation (1) may break at some points or in some subset in the state space as the next example shows. This pathological situation occurs by making an oversimplified model for a real physical circuit. It can be remedied, however, by an appropriate normalization technique, such as inserting stray reactance elements into suitable positions of the circuit.

Example 2. In Eq. (7), if we remove the capacitor (i.e., $C = 0$), then we have

$$\begin{aligned} i &= -g_1v + g_3v^3\\ L\frac{di}{dt} &= -v\end{aligned} \tag{26}$$

By eliminating i, we have the state equation:

$$L(g_1 - 3g_3v^2)\frac{dv}{dt} = v \tag{27}$$

or equivalently

$$\frac{dv}{dt} = \frac{v}{L(g_1 - 3g_3v^2)} \tag{28}$$

Hence at the point $v^2 = g_1/3g_3$, Eq. (27) or (28) becomes singular; that is, the circuit dynamics could not be defined. Note that, instead of the inductor's current i, the conductor's voltage is used for describing Eq. (27). The inductor is connected in series with the voltage-controlled conductor with noninvertible characteristics. Hence even if the element characteristics are differentiable, the state equation can never be described by the normal form of Eq. (1). The above points are called *impasse points* and generally appear by making an oversimplification of a mathematical model of the circuit. Indeed if we consider a small stray capacitance C in parallel with the nonlinear conductor, then the state equation is written in the form of Eq. (4).

Continuous Dependence on Initial Condition and Parameters at a Finite Time

Knowing that the solution Eq. (21) exists for any initial state and parameters, we can regard the solution Eq. (21) as the following function:

$$\varphi(t, \cdot, \cdot): \quad \mathbf{R}^n \times \mathbf{R}^m \to \mathbf{R}^n; \quad (\mathbf{x}_0, \lambda) \mapsto \varphi(t, \mathbf{x}_0, \lambda) \tag{29}$$

Hence we can find the continuity and the differentiability of the solution with respect to $\mathbf{x}_0$ and λ. Roughly speaking, the dependence of the solution Eq. (29) on $(\mathbf{x}_0, \lambda)$ is as continuous as the function $\mathbf{f}$. Hence we have the following result.

Theorem 2. Suppose the function $\mathbf{f}(t, \mathbf{x}, \lambda)$ of Eq. (1) is differentiable, then the solution Eq. (21) is also differentiable with respect to the initial state $\mathbf{x}_0$ and system parameter λ. In fact the matrices $\partial\varphi(t, \mathbf{x}_0, \lambda)/\partial\mathbf{x}_0$ and $\partial\varphi(t, \mathbf{x}_0, \lambda)/\partial\lambda$ exist and they satisfy the linear matrix differential equations:

$$\frac{d}{dt}\frac{\partial\varphi(t, \mathbf{x}_0, \lambda)}{\partial\mathbf{x}_0} = \frac{\partial\mathbf{f}(t, \varphi(t, \mathbf{x}_0, \lambda), \lambda)}{\partial\mathbf{x}}\frac{\partial\varphi(t, \mathbf{x}_0, \lambda)}{\partial\mathbf{x}_0} \tag{30}$$

$$\frac{d}{dt}\frac{\partial\varphi(t, \mathbf{x}_0, \lambda)}{\partial\lambda} = \frac{\partial\mathbf{f}(t, \varphi(t, \mathbf{x}_0, \lambda), \lambda)}{\partial\mathbf{x}}\frac{\partial\varphi(t, \mathbf{x}_0, \lambda)}{\partial\lambda} + \frac{\partial\mathbf{f}(t, \varphi(t, \mathbf{x}_0, \lambda), \lambda)}{\partial\lambda} \tag{31}$$

with the initial conditions

$$\frac{\partial\varphi(t_0, \mathbf{x}_0, \lambda)}{\partial\mathbf{x}_0} = \mathbf{I}_n \tag{32}$$

$$\frac{\partial\varphi(t_0, \mathbf{x}_0, \lambda)}{\partial\lambda} = \mathbf{0} \tag{33}$$

respectively, where $\mathbf{I}_n$ is the $n \times n$ identity matrix. Equations (30) and (31) are called the linear variational equations with respect to the initial condition and the system parameters, respectively.

Remark 3. 1. This result can be easily proved by differentiating Eqs. (22) and (23) with respect to $\mathbf{x}_0$ and λ.

2. The variational equation Eq. (30) is derived another way as follows. Suppose that we want to know a neighboring solution of the solution Eq. (21). By considering a small variation $\xi(t)$ from Eq. (21) as

$$\mathbf{x}(t) = \varphi(t, \mathbf{x}_0, \lambda) + \xi(t) \tag{34}$$

and substituting this into Eq. (1), we have

$$\begin{aligned}\dot{\varphi}(t, \mathbf{x}_0, \lambda) + \dot{\xi}(t) &= \mathbf{f}(t, \varphi(t, \mathbf{x}_0, \lambda) + \xi(t), \lambda) \\ &= \mathbf{f}(t, \varphi(t, \mathbf{x}_0, \lambda), \lambda) \\ &\quad + \frac{\partial\mathbf{f}(t, \varphi(t, \mathbf{x}_0, \lambda), \lambda)}{\partial\mathbf{x}}\xi(t) + \cdots\end{aligned}$$

where . . . denotes the higher-order terms of $\xi(t)$. Comparing both sides of this equation and neglecting the higher-order terms, we have a linear equation

$$\dot{\xi}(t) = \frac{\partial\mathbf{f}(t, \varphi(t, \mathbf{x}_0, \lambda), \lambda)}{\partial\mathbf{x}}\xi(t) \tag{35}$$

The initial value $\xi(t_0) = \xi_0$ at $t = t_0$ is the initial variation from the initial state $\mathbf{x}_0$. The same argument is applied to Eq. (31) for the system parameter λ.

3. Second- and higher-order derivatives with respect to $\mathbf{x}_0$ and λ can be obtained similarly by differentiating Eqs. (30)–(33). These higher-order derivatives give useful information when we will consider the bifurcation problem of a specific steady state.

Structure of Circuit Dynamics

As stated earlier, a circuit usually consists of three kinds of circuit elements: capacitors, inductors, and resistors. If one of these types of circuit elements is never used in a circuit, the circuit dynamics becomes a particular type of dynamical system. For example, dynamics of a circuit containing only capacitors and resistors has a special form called a *gradient system.* A similar situation occurs in a circuit with another combination of circuit elements. We illustrate some types of dynamical systems which arise also in other physical systems.

Gradient System. A gradient system is a system whose vector field is defined by the gradient of a scalar function of state. Let F be a scalar function, also called a *potential* or *dissipative* function:

$$F: \quad \mathbf{R}^n \to \mathbf{R}; \mathbf{x} \mapsto F(\mathbf{x}) \tag{36}$$

A system of the form

$$\dot{\mathbf{x}} = -gradF(\mathbf{x}) \tag{37}$$

is called a gradient system, where

$$gradF(\mathbf{x}) = \left(\frac{\partial F}{\partial\mathbf{x}}\right)^T = \left(\frac{\partial F}{\partial x_1}, \cdots, \frac{\partial F}{\partial x_n}\right)^T \tag{38}$$

and $(\,)^T$ denotes the transpose of the derivative vector $\partial F/\partial\mathbf{x}$. In gradient system, F always decreases along a trajectory $\mathbf{x}(t)$. That is the total time derivative of F is negative or zero:

$$\frac{dF}{dt} = \frac{\partial F}{\partial\mathbf{x}}\frac{d\mathbf{x}}{dt} = -\frac{\partial F}{\partial\mathbf{x}}\left(\frac{\partial F}{\partial\mathbf{x}}\right)^T \le 0 \tag{39}$$

Hamiltonian System, Conservative System, or Lossless System. In classical mechanics we study mainly Hamiltonian systems. In circuit application, a lossless circuit is described by this type of equation. Let an energy function H be defined as

$$H: \quad \mathbf{R}^n \times \mathbf{R}^n \to \mathbf{R};\ (\mathbf{x}, \mathbf{y}) \mapsto H(\mathbf{x}, \mathbf{y}) \tag{40}$$

A system of the form

$$\dot{\mathbf{x}} = \left(\frac{\partial H}{\partial \mathbf{y}}\right)^T, \qquad \dot{\mathbf{y}} = -\left(\frac{\partial H}{\partial \mathbf{x}}\right)^T \tag{41}$$

is called a Hamiltonian system with n degrees of freedom. In Hamiltonian system H remains constant along a trajectory of Eq. (41).

$$\frac{dH}{dt} = \frac{\partial H}{\partial \mathbf{x}}\frac{d\mathbf{x}}{dt} + \frac{\partial H}{\partial \mathbf{y}}\frac{d\mathbf{y}}{dt} = \frac{\partial H}{\partial \mathbf{x}}\left(\frac{\partial H}{\partial \mathbf{y}}\right)^T - \frac{\partial H}{\partial \mathbf{y}}\left(\frac{\partial H}{\partial \mathbf{x}}\right)^T = 0 \tag{42}$$

Thus, H is constant along any solution curve of Eq. (41) and the trajectories lie on the surfaces H = constant. This property is called the *conservation of energy.*

Dissipative System. A dissipative system is a combined system of the above two systems. Let F be a dissipative scalar function:

$$F: \quad \mathbf{R}^n \times \mathbf{R}^n \to \mathbf{R};\ (\mathbf{x}, \mathbf{y}) \mapsto F(\mathbf{x}, \mathbf{y}) \tag{43}$$

and let H be an energy function of the form Eq. (40).

A system of the form

$$\dot{\mathbf{x}} = \left(\frac{\partial H}{\partial \mathbf{y}}\right)^T - \left(\frac{\partial F}{\partial \mathbf{x}}\right)^T, \quad \dot{\mathbf{y}} = -\left(\frac{\partial H}{\partial \mathbf{x}}\right)^T - \left(\frac{\partial F}{\partial \mathbf{y}}\right)^T \tag{44}$$

is called a *dissipative system.* Here for simplicity we define a typical dissipative system by assuming two states variables $\mathbf{x}$ and $\mathbf{y}$ have the same dimension n.

Example 3. 1. *An RC circuit.* Consider the circuit shown in Fig. 6. We assume that the nonlinear conductors g_1 and g_2 are voltage-controlled and have the same characteristics as

$$i_{gl} = g(v_l) = -g_1 v_l + g_3 v_l^3 \qquad (l = 1, 2) \tag{45}$$

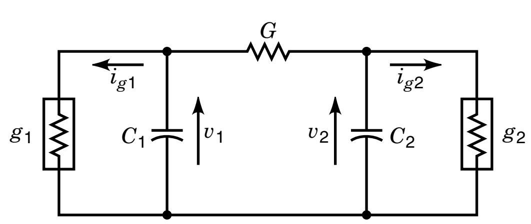

Figure 6. *RC* circuit with nonlinear resistors.

Following the notation in the figure, we have the state equation:

$$\begin{aligned} C_1\frac{dv_1}{dt} &= -g(v_1) - G(v_1 - v_2) \\ C_2\frac{dv_2}{dt} &= -g(v_2) - G(v_2 - v_1) \end{aligned} \tag{46}$$

Defining the dissipative function

$$F(v_1, v_2) = \frac{1}{2}G(v_1 - v_2)^2 + \int_0^{v_1} g(v_1)dv_1 + \int_0^{v_2} g(v_2)dv_2 \tag{47}$$

Eq. (46) can be rewritten as

$$\begin{aligned} C_1\frac{dv_1}{dt} &= -\frac{\partial F(v_1, v_2)}{\partial v_1} \\ C_2\frac{dv_2}{dt} &= -\frac{\partial F(v_1, v_2)}{\partial v_2} \end{aligned} \tag{48}$$

Hence Eq. (48) is a kind of gradient system. In fact, F decreases along a trajectory, that is,

$$\begin{aligned} \frac{dF}{dt} &= \frac{\partial F}{\partial v_1}\frac{dv_1}{dt} + \frac{\partial F}{\partial v_2}\frac{dv_2}{dt} \\ &= -\left\{\frac{1}{C_1}\left(\frac{\partial F}{\partial v_1}\right)^2 + \frac{1}{C_2}\left(\frac{\partial F}{\partial v_2}\right)^2\right\} \leqq 0 \end{aligned} \tag{49}$$

More generally we can prove that any *RC* circuit, similarly any *RL* circuit, is a dissipative system. In the case of $C_1 = C_2 = C$, Eq. (46) becomes a symmetrical system. That is, Eq. (46) is invariant under the linear coordinate transformations:

$$\sigma_1: \quad \mathbf{R}^2 \to \mathbf{R}^2; \quad (v_1, v_2) \mapsto \sigma_1(v_1, v_2) = (v_2, v_1) \tag{50}$$

and

$$\iota: \quad \mathbf{R}^2 \to \mathbf{R}^2; \quad (v_1, v_2) \mapsto \iota(v_1, v_2) = (-v_1, -v_2) \tag{51}$$

Hence Eq. (46) is invariant under the composition of the above transformations:

$$\sigma_2 = \iota \circ \sigma_1: \quad \mathbf{R}^2 \to \mathbf{R}^2; \quad (v_1, v_2) \mapsto \sigma_2(v_1, v_2) = (-v_2, -v_1) \tag{52}$$

Thus the above three linear transformations are expressed by the following matrices:

$$\sigma_1 = \begin{bmatrix} 0 & 1 \\ 1 & 0 \end{bmatrix}, \qquad \iota = \begin{bmatrix} -1 & 0 \\ 0 & -1 \end{bmatrix}, \qquad \sigma_2 = \begin{bmatrix} 0 & -1 \\ -1 & 0 \end{bmatrix} \tag{53}$$

With the identity matrix $\mathbf{I}_2$, they form a transformation group. Under these transformations we have two invariant subspaces:

$$\begin{aligned} E_1 &= \{(v_1, v_2) \in \mathbf{R}^2 \mid v_1 = v_2\} \\ E_2 &= \{(v_1, v_2) \in \mathbf{R}^2 \mid v_1 = -v_2\} \end{aligned} \tag{54}$$

In these subspaces, each solution of Eq. (48) remains in the same subspace and the dynamics becomes one-dimensional systems, that is,

$$
\begin{aligned}
C\frac{dv}{dt} &= -g(v), \qquad v \in E_1 \\
C\frac{dv}{dt} &= -g(v) - 2Gv, \qquad v \in E_2
\end{aligned}
\tag{55}
$$

2. *An LC circuit.* Consider the circuit discussed in Example 1(2) with $R = 0$. The circuit becomes a lossless circuit, so that it becomes a Hamiltonian system. In fact we define the Hamiltonian:

$$H(v_C, \phi) = \frac{1}{2n}v_C^2 + \frac{1}{nC}F(\phi) - \frac{v_C E}{n}\sin\omega t \tag{56}$$

where

$$F(\phi) = \int_0^\phi f(\phi)\, d\phi = \frac{1}{2}a_1\phi^2 + \frac{1}{3}a_2\phi^3 + \frac{1}{4}a_3\phi^4 \tag{57}$$

then we have Eq. (17) as

$$
\begin{aligned}
\frac{dv_C}{dt} &= \frac{\partial H}{\partial \phi} = \frac{1}{nC}f(\phi) \\
\frac{d\phi}{dt} &= -\frac{\partial H}{\partial v_C} = -\frac{1}{n}v_C + \frac{E}{n}\sin\omega t
\end{aligned}
\tag{58}
$$

On the other hand, if we define

$$H(x, y) = \frac{1}{2}y^2 + \frac{1}{2}c_1x^2 + \frac{1}{4}c_3x^4 - x(B_0 + B\cos\tau) \tag{59}$$

then we obtain Eq. (20) as

$$
\begin{aligned}
\frac{dx}{d\tau} &= \frac{\partial H}{\partial y} = y \\
\frac{dy}{d\tau} &= -\frac{\partial H}{\partial x} = -c_1x - c_3x^3 + B_0 + B\cos\tau
\end{aligned}
\tag{60}
$$

In both cases, the Hamiltonian is a periodic function in time.

3. *An RLC circuit.* Equation (11) in Example 1(1) is a dissipative system. To see this, define the energy function:

$$H(x, y) = \frac{1}{2}y^2 + \frac{1}{2}x^2 \tag{61}$$

and the dissipative function:

$$F(x, y) = -\frac{1}{2}\gamma_1x^2 + \frac{1}{4}\gamma_4x^4 + \frac{1}{2}ky^2 - By \tag{62}$$

then, we have Eq. (17) as

$$
\begin{aligned}
\frac{dx}{d\tau} &= \frac{\partial H}{\partial y} - \frac{\partial F}{\partial x} \\
\frac{dy}{d\tau} &= -\frac{\partial H}{\partial x} - \frac{\partial F}{\partial y}
\end{aligned}
\tag{63}
$$

Hence the energy dissipation along a trajectory is

$$\frac{dH}{d\tau} = \frac{\partial H}{\partial x}\frac{dx}{d\tau} + \frac{\partial H}{\partial y}\frac{dy}{d\tau} = -(-\gamma_1x^2 + \gamma_3x^4 - By + ky^2) \tag{64}$$

which will be negative for sufficiently large $(x, y) \in \mathbf{R}^2$.

References in This Section

For ordinary differential equations there are many excellent books. We refer to only some of them (10–12). For the normal form of general nonlinear circuits, see Refs. 5 and 13. The circuit shown in Example 1(1) is found in Refs. 11 and 14, where in the latter the circuit dynamics Eq. (11) is called the Bonhoeffer van der Pol equation (BVP equation). The circuit shown in Example 1(2) is found in Ref. 3. For the impasse points and related topics, see Refs. 15 and 16. Similar circuit shown in Example 3(a) is found in Ref. 1 as two dynamos working in parallel on a common load. For the gradient system, see Ref. 12, and for the Hamiltonian systems, see Refs. 7 and 8.

LOCAL PROPERTIES OF CIRCUIT DYNAMICS

The qualitative, geometrical, or topological approach of nonlinear ordinary differential equations is a powerful tool for understanding the nonlinear phenomena of circuit dynamics. In this and the following sections we introduce some basic examples from this approach. For now we consider an autonomous system

$$\dot{\mathbf{x}} = \mathbf{f}(\mathbf{x}, \lambda), \qquad \mathbf{x} \in \mathbf{R}^n,\ \lambda \in \mathbf{R}^m \tag{65}$$

where $\mathbf{x} \in \mathbf{R}^n$ is a state vector and $\lambda \in \mathbf{R}^m$ is a system parameter. Usually the terms "state" and "phase" have the same meaning. Hence the state space $\mathbf{R}^n$ is also called the phase space. In the two-dimensional case, we say the phase plane instead of the state plane. Note that Eq. (65) defines the phase velocity vector field at every point in the phase space. The phase portrait of Eq. (65) is the set of all trajectories in the phase space $\mathbf{R}^n$. The phase portrait contains useful information of the behavior of trajectories. We see the number and types of equilibrium points, their asymptotic behavior when $t \to \pm\infty$, and so on. In practice, only typical trajectories are illustrated in the portrait to show the behavior schematically.

Equilibrium Point and its Topological Classification

A point at which the phase velocity becomes zero is called an *equilibrium point.* The point corresponds to a dc operating point of a circuit. Hence an equilibrium point $\mathbf{x}_0 \in \mathbf{R}^n$ is given by the relation

$$\mathbf{f}(\mathbf{x}_0, \lambda) = \mathbf{0} \tag{66}$$

For every equilibrium point the solution

$$\mathbf{x}(t) = \mathbf{x}_0 \tag{67}$$

gives a stationary solution of Eq. (65).

Example 4. 1. Consider Eq. (11) in Example 1(1). Equation (66) is given by

$$
\begin{aligned}
f_1(x_0, y_0) &= y_0 + \gamma_1x_0 - \gamma_3x_0^3 = 0 \\
f_2(x_0, y_0) &= -x_0 - ky_0 + B = 0
\end{aligned}
\tag{68}
$$

The intersection of these two curves gives a solution of Eq. (68). Hence by choosing parameters appropriately we see that at most three equilibria exist in Eq. (68). Substituting the first equation into the second, we find

$$(1 - k\gamma_1)x_0 + k\gamma_3 x_0^3 = B \tag{69}$$

Hence, if $1 < k\gamma_1$, then for $|B| < \frac{2}{3}(k\gamma_1 - 1)\sqrt{(k\gamma_1 - 1)/3k\gamma_3}$ Eq. (69) has three roots. For example, if $B = 0$, then we have three equilibria:

$$\left(-\sqrt{\frac{k\gamma_1 - 1}{k\gamma_3}}, \frac{1}{k}\sqrt{\frac{k\gamma_1 - 1}{k\gamma_3}}\right), \quad (0, 0), \quad \left(\sqrt{\frac{k\gamma_1 - 1}{k\gamma_3}}, -\frac{1}{k}\sqrt{\frac{k\gamma_1 - 1}{k\gamma_3}}\right) \tag{70}$$

For $1 > k\gamma_1$ Eq. (69) has only one equilibrium point.

2. Consider Eq. (13) or Eq. (14) in Example 1(1). If γ_1 and γ_3 are positive, then the origin $(x, \dot{x}) = (0, 0)$ in Eq. (13), or $(y, \dot{y}) = (0, 0)$ in Eq. (14) is the unique equilibrium point of the systems.

3. Consider the circuit shown in Fig. 7. Using the notation in the figure we have the circuit equation:

$$\begin{aligned} L_1\frac{di_1}{dt} &= E_1 - R_1 i_1 - v \\ L_2\frac{di_2}{dt} &= E_2 - R_2 i_2 - v \\ C\frac{dv}{dt} &= i_1 + i_2 - g(v) \end{aligned} \tag{71}$$

where the nonlinear characteristics of the conductor G is assumed as

$$i_G(v_G) = -g_1 v_G + g_3 v_G^3, \quad g_1, g_3 > 0 \tag{72}$$

Hence the equilibrium point is given by

$$\begin{aligned} f_1(i_1, i_2, v) &= E_1 - R_1 i_1 - v = 0 \\ f_2(i_1, i_2, v) &= E_2 - R_2 i_2 - v = 0 \\ f_3(i_1, i_2, v) &= i_1 + i_2 - g(v) = 0 \end{aligned} \tag{73}$$

Substituting the first and second equations into the third equation, we have the following cubic function of v:

$$f(v) = \frac{E_1}{R_1} + \frac{E_2}{R_2} - \left(\frac{1}{R_1} + \frac{1}{R_2} - g_1\right)v - g_3 v^3 = 0 \tag{74}$$

Hence Eq. (73) has at most three equilibria under appropriate parameter values.

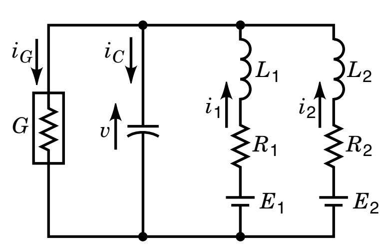

Figure 7. A three-dimensional oscillatory circuit.

Once we have an equilibrium point $\mathbf{x}_0$, our interest turns into its stability or the qualitative property of the behavior of trajectories near $\mathbf{x}_0$. To do this let ξ be a small variation from the equilibrium point:

$$\mathbf{x}(t) = \mathbf{x}_0 + \xi(t) \tag{75}$$

Substituting Eq. (75) into Eq. (65), we have the linear variational equation as

$$\dot{\xi}(t) = \mathbf{A}\xi(t) \tag{76}$$

where $\mathbf{A} = D\mathbf{f}(\mathbf{x}_0, \lambda)$ is the Jacobian matrix with respect to $\mathbf{x}$ at $\mathbf{x}_0$. Equation (76) gives also the linear approximation of the original system (65) in the neighborhood of the equilibrium point $\mathbf{x}_0$. Indeed by Taylor's expansion we have

$$\mathbf{f}(\mathbf{x}_0 + \xi, \lambda) = D\mathbf{f}(\mathbf{x}_0, \lambda)\xi + \frac{1}{2}D^2\mathbf{f}(\mathbf{x}_0, \lambda)(\xi, \xi) + \cdots \tag{77}$$

It follows that the linear part $\mathbf{A}\xi = D\mathbf{f}(\mathbf{x}_0, \lambda)\xi$ is a good approximation to the nonlinear function $\mathbf{f}(\cdot, \lambda)$ near the equilibrium point $\mathbf{x} = \mathbf{x}_0$, and it is reasonable to expect that the qualitative behavior of Eq. (65) near $\mathbf{x} = \mathbf{x}_0$ will be approximated by the behavior of Eq. (76). This is indeed the case if the matrix $\mathbf{A} = D\mathbf{f}(\mathbf{x}_0, \lambda)$ has no zero or pure imaginary eigenvalues. Hence we define an equilibrium point with this condition as a hyperbolic equilibrium point. That is, an equilibrium point is hyperbolic if none of the eigenvalues of the matrix $\mathbf{A} = D\mathbf{f}(\mathbf{x}_0, \lambda)$ have zero real part. The Hartman–Grobman theorem shows that near a hyperbolic equilibrium point, the nonlinear system of Eq. (65) has the same qualitative structure as the linear system of Eq. (76). That is, by a homeomorphism (continuous mapping with its inverse) h from an open set U containing $\mathbf{x}_0$ of Eq. (65) onto an open set V containing the origin of Eq. (76), trajectories of Eq. (65) in U map onto trajectories of Eq. (76) while preserving their orientation by time. Here "qualitative structure," "topological property," or "topological type" has the same meaning.

Using this result, we can classify topologically hyperbolic equilibrium point. Let

$$\chi(\mu) = \det[\mu\mathbf{I}_n - D\mathbf{f}(\mathbf{x}_0, \lambda)] = 0 \tag{78}$$

be the characteristic equation and let

$$\{\mu_1, \mu_2, \cdots, \mu_n\} = \{\mu_i \in \mathbf{C} \mid \det[\mu_i\mathbf{I}_n - D\mathbf{f}(\mathbf{x}_0, \lambda)] = 0\} \tag{79}$$

be the eigenvalues, also called the characteristic roots, of $\mathbf{A} = D\mathbf{f}(\mathbf{x}_0, \lambda)$. Then the hyperbolic condition is given by

$$\mathrm{Re}(\mu_i) \neq 0 \tag{80}$$

for all $i = 1, 2, \ldots, n$. Now let $\mathbf{E}^u$ be the intersection of $\mathbf{R}^n$ and the direct sum of generalized eigenspace of $\mathbf{A}$ corresponding to the eigenvalues μ_i such that $\mathrm{Re}(\mu_i) > 0$. Similarly, let $\mathbf{E}^s$ be the intersection of $\mathbf{R}^n$ and the direct sum of generalized eigenspace of $\mathbf{A}$ corresponding to the eigenvalues μ_i such that $\mathrm{Re}(\mu_i) < 0$. $\mathbf{E}^u$ or $\mathbf{E}^s$ is called the unstable or stable subspace of $\mathbf{A}$. The Hartman–Grobman theorem shows that $\mathbf{E}^u$ and $\mathbf{E}^s$

have the following properties:

$$\begin{aligned}&\text{(a) } \mathbf{R}^n = \mathbf{E}^u \oplus \mathbf{E}^s, \qquad \mathbf{A}(\mathbf{E}^u) = \mathbf{E}^u, \mathbf{A}(\mathbf{E}^s) = \mathbf{E}^s \\ &\text{(b) } \dim \mathbf{E}^u = \#\{\mu_i \mid \mathrm{Re}(\mu_i) > 0\}, \\ &\qquad \dim \mathbf{E}^s = \#\{\mu_i \mid \mathrm{Re}(\mu_i) < 0\}\end{aligned} \tag{81}$$

where #{ } indicates the number of the elements contained in the set { }. The topological type of a hyperbolic equilibrium point is then determined by the dim $\mathbf{E}^u$ or dim $\mathbf{E}^s$. Let ${}_kO$ denotes the topological type of a hyperbolic equilibrium point with dim $\mathbf{E}^u = k$. That is, ${}_kO$ denotes the type of a k-dimensionally unstable hyperbolic equilibrium point. Then for the n-dimensional autonomous system Eq. (65) we have $n + 1$ topologically different kinds of hyperbolic equilibria. Their types are as follows:

$$\{{}_0O,\ {}_1O, \cdots,\ {}_nO\} \tag{82}$$

Usually a completely stable equilibrium point ${}_0O$ is called a *sink,* a completely unstable equilibrium point ${}_nO$ is called a *source,* and others are called *saddles.*

Remark 4. 1. *Stability of equilibrium point.* The stability of any hyperbolic equilibrium point $\mathbf{x}_0 \in \mathbf{R}^n$ is determined by the signs of the real parts of the characteristic roots Eq. (79). A hyperbolic equilibrium point $\mathbf{x}_0 \in \mathbf{R}^n$ is called *asymptotically stable* if and only if it is a sink: $\mathrm{Re}(\mu_i) < 0$ for all $i = 1, 2, \ldots, n$. A hyperbolic equilibrium point is unstable if it is a source or a saddle. The stability of nonhyperbolic equilibrium point is more difficult to determine. The definition of the stability due to Lyapunov is useful for this purpose. Let $\varphi(t, \mathbf{u}, \lambda)$ be a solution of Eq. (65) with $\varphi(0, \mathbf{u}, \lambda) = \mathbf{u}$. An equilibrium point $\mathbf{x}_0$ is stable (in the sense of Lyapunov) if for every $\epsilon > 0$ there exists a $\delta > 0$ such that for every $\mathbf{u} \in B(\delta, \mathbf{x}_0)$ we have $\varphi(t, \mathbf{x}_0, \lambda) \in B(\epsilon, \mathbf{x}_0)$ for all $t \geq 0$, where $B(d, \mathbf{x}_0)$ denotes an open disk with the radius d: $B(d, \mathbf{x}_0) = \{\mathbf{u} \in \mathbf{R}^n \mid \|\mathbf{u} - \mathbf{x}_0\| < d\}$. An equilibrium point $\mathbf{x}_0$ is unstable if it is not stable. And $\mathbf{x}_0$ is asymptotically stable if it is stable and $\lim_{t\to\infty} \varphi(t, \mathbf{x}_0, \lambda) = \mathbf{x}_0$. An asymptotic stable equilibrium point is the simplest attractor of dynamical systems.

2. *Stable and unstable manifolds of a hyperbolic equilibrium point.* The subsets leaving from and approaching to a hyperbolic equilibrium point $\mathbf{x}_0$ are called the unstable manifold $W^s(\mathbf{x}_0)$ and the stable manifold $W^u(\mathbf{x}_0)$, respectively. They are defined as

$$\begin{aligned}W^u(\mathbf{x}_0) &= \{\mathbf{u} \in \mathbf{R}^n \mid \lim_{t\to-\infty} \varphi(t, \mathbf{u}, \lambda) = \mathbf{x}_0\} \\ W^s(\mathbf{x}_0) &= \{\mathbf{u} \in \mathbf{R}^n \mid \lim_{t\to\infty} \varphi(t, \mathbf{u}, \lambda) = \mathbf{x}_0\}\end{aligned} \tag{83}$$

$\mathbf{E}^u$ and $\mathbf{E}^s$ defined in Eq. (81) are tangent spaces to $W^u(\mathbf{x}_0)$ and $W^s(\mathbf{x}_0)$ at $\mathbf{x}_0$, and

$$\begin{aligned}&\dim\mathbf{E}^u = \dim W^u(\mathbf{x}_0), \qquad \dim\mathbf{E}^s = \dim W^s(\mathbf{x}_0), \\ &W^u(\mathbf{x}_0) \cap W^s(\mathbf{x}_0) = \mathbf{x}_0\end{aligned} \tag{84}$$

3. Let $\varphi(t, \mathbf{x}_0, \lambda)$ be a solution of Eq. (65) with $\varphi(0, \mathbf{x}_0, \lambda) = \mathbf{x}_0$. The curve traced out the trajectory $\varphi(t, \mathbf{x}_0, \lambda)$:

$$Orb(\mathbf{x}_0) = \{\mathbf{x} \in \mathbf{R}^n \mid \mathbf{x} = \varphi(t, \mathbf{x}_0, \lambda), t \in \mathbf{R}\} \tag{85}$$

is called the orbit of Eq. (65) through the initial state $\mathbf{x}_0$. Asymptotic behavior in the future or in the past is also defined as

$$\begin{aligned}\omega(\mathbf{x}_0) &= \omega(Orb(\mathbf{x}_0)) = \omega\lim(\mathbf{x}_0) = \bigcap_{\tau\geq 0} \overline{\bigcup_{t\geq\tau} \varphi(t, \mathbf{x}_0, \lambda)} \\ \alpha(\mathbf{x}_0) &= \alpha(Orb(\mathbf{x}_0)) = \alpha\lim(\mathbf{x}_0) = \bigcap_{\tau\leq 0} \overline{\bigcup_{t\leq\tau} \varphi(t, \mathbf{x}_0, \lambda)}\end{aligned} \tag{86}$$

They are called the ω limit set and the α limit set of $\mathbf{x}_0$ or $Orb(\mathbf{x}_0)$, respectively. Now suppose that $\mathbf{p} \in \mathbf{R}^n$ be a sink. Then the set of all point $\mathbf{x}_0$ whose ω limit set is $\mathbf{p}$ is called the basin of attraction or the domain of attraction of the attractor $\mathbf{p}$:

$$Basin(\mathbf{p}) = \{\mathbf{x} \in \mathbf{R}^n \mid \omega\lim(\mathbf{x}) = \mathbf{p}\} \tag{87}$$

If a system has several stable equilibria as attractors, then each attractor has its own basin of attraction. The state space considered as the set of initial states is divided into their basins of attractors. Hence the final steady state realized is completely determined by the basin in which we specify an initial state. This is the simplest nonlinear phenomenon of the existence of multistable states.

Example 5. 1. *Two-dimensional hyperbolic equilibria.* We have three different types of hyperbolic equilibria: ${}_0O$, ${}_1O$, ${}_2O$. Assume that the characteristic equation Eq. (78) is given by

$$\chi(\mu) = \det[\mu\mathbf{I}_2 - D\mathbf{f}(\mathbf{x}_0, \lambda)] = \mu^2 + a_1\mu + a_2 = 0 \tag{88}$$

Then we have the following result:

(a) If $a_1 > 0$ and $a_2 > 0$, then the equilibrium point $\mathbf{x}_0 \in \mathbf{R}^2$ is a sink ${}_0O$.

(b) If $a_2 < 0$, then the equilibrium point $\mathbf{x}_0 \in \mathbf{R}^2$ is a saddle ${}_1O$.

(c) If $a_1 < 0$ and $a_2 > 0$, then the equilibrium point $\mathbf{x}_0 \in \mathbf{R}^2$ is a source ${}_2O$.

These relations are illustrated in Fig. 8. Each type of hyperbolic equilibrium point is also classified by the location of its

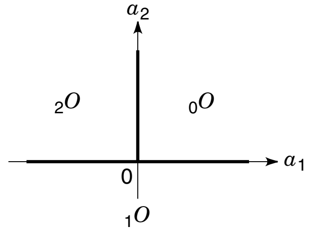

Figure 8. Topological classification of equilibria: two-dimensional case.

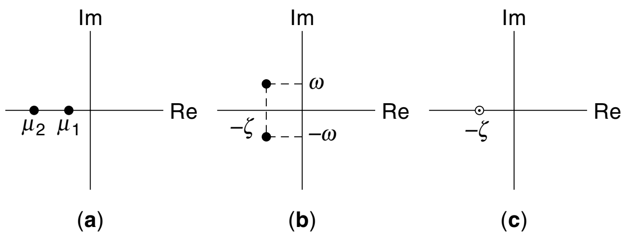

Figure 9. Distribution of the characteristic roots for a sink.

characteristic roots in the plane of complex numbers. Figure 9 shows the typical locations of a sink. Corresponding to these roots, we have the phase portraits shown in Fig. 10. The equilibrium point of each case is called a node in Fig. 9(a), a spiral or a focus in Fig. 9(b), and a degenerate focus in Fig. 9(c). Note that for the multiple roots, we have two types of degenerate focuses shown in (c-1) and (c-2) in Fig. 10. Figure 11 shows the location of characteristic roots for a saddle point (a) and its phase portrait (b). In a two-dimensional system, two cases occur for a nonhyperbolic equilibrium point: (a) characteristic roots are pure imaginary numbers, and (b) one root is zero. These nonhyperbolic equilibria are called center and degenerate node, respectively, (see Fig. 12).

2. *Consider the van der Pol equation in Example 1(1).* Equation (13) is rewritten as

$$\begin{aligned} \dot{x} &= y \\ \dot{y} &= -x + \epsilon(1 - \gamma x^2)y \end{aligned} \tag{89}$$

where

$$\epsilon = \gamma_1 > 0, \qquad \gamma = 3\frac{\gamma_3}{\gamma_1} > 0 \tag{90}$$

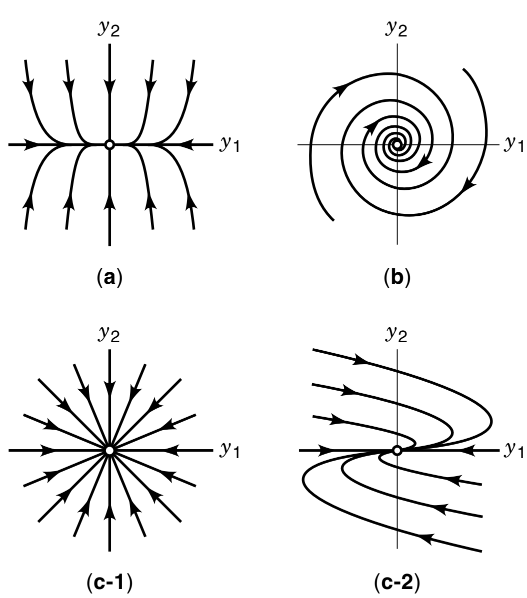

Figure 10. Phase portrait of a sink. (a) Node, (b) focus, (c) degenerate focus.

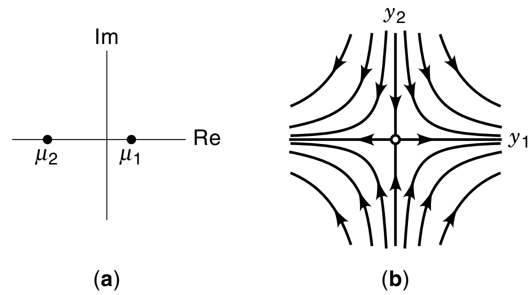

Figure 11. Distribution of the characteristic roots for (a) a saddle and (b) a phase portrait of a saddle.

The only equilibrium point is the origin. The characteristic equation of the origin is given by

$$\chi(\mu) = \begin{vmatrix} -\mu & 1 \\ -1 & \epsilon - \mu \end{vmatrix} = \mu^2 - \epsilon\mu + 1 = 0 \tag{91}$$

Hence the origin is a source ${}_2O$, that is, a two-dimensionally unstable hyperbolic equilibrium point.

3. *The existence of multistable states.* Consider Eq. (46) with $C_1 = C_2 = C$:

$$\begin{aligned} \dot{x} &= \alpha x - x^3 - \delta(x - y) \\ \dot{y} &= \alpha y - y^3 - \delta(y - x) \end{aligned} \tag{92}$$

where we put

$$v_1 = \sqrt{\frac{C}{g_3}}x, \quad v_2 = \sqrt{\frac{C}{g_3}}y, \quad \alpha = \frac{g_1}{C} > 0, \quad \delta = \frac{G}{C} > 0 \tag{93}$$

These two equations have the mirror reflection symmetry with respect to the invariant subspaces given by Eq. (54), that is, $x = y$ and $x = -y$. In the case of $\alpha = 4$, $\delta = 1$ we have nine equilibria as shown in Fig. 13. Note that the stationary points of the dissipative function in Eq. (47) give these equilibria (see Fig. 14). The Jacobian matrix at an equilibrium point (x_0, y_0) is given by

$$\mathbf{A} = D\mathbf{f}(x_0, y_0) = \begin{bmatrix} \alpha - \delta - 3x_0^2 & \delta \\ \delta & \alpha - \delta - 3y_0^2 \end{bmatrix} \tag{94}$$

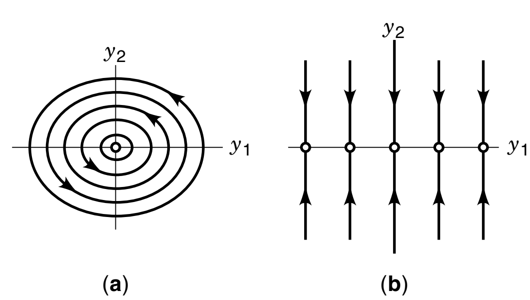

Figure 12. Phase portrait of nonhyperbolic equilibrium point. (a) Center, (b) degenerate node.

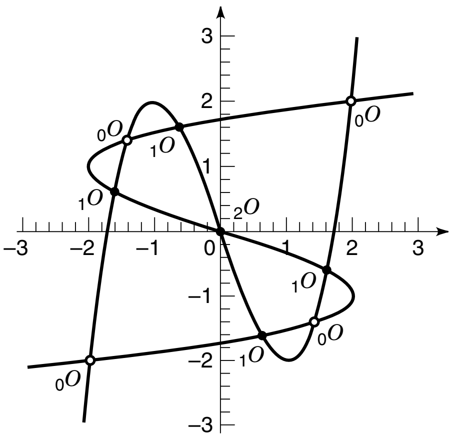

Figure 13. Equilibria for Eq. (92) with $\alpha = 4$ and $\delta = 1$.

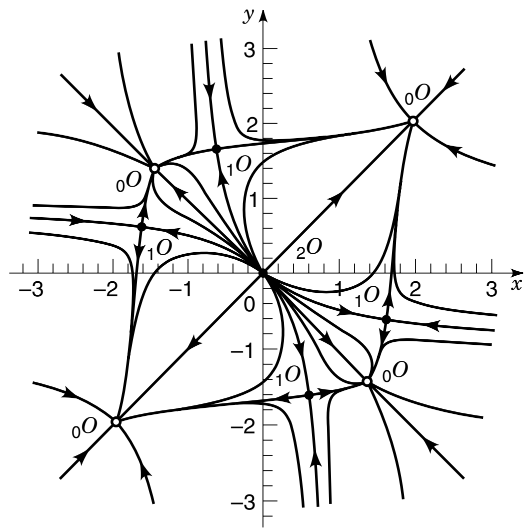

Figure 15. Phase portrait of Eq. (92) with $\alpha = 4$ and $\delta = 1$.

All equilibria are hyperbolic and their types are easily calculated from Eq. (94). The phase portrait is illustrated in Fig. 15. Stable manifolds approaching four saddle points separate the phase plane into four regions in which one sink is situated. That is, the phase plane is divided into four basins of attractions whose boundaries are stable manifolds of the saddle points.

References in This Section

A qualitative approach of ordinary differential equations or dynamical systems is found in Refs. 1, 4, 7, and 9. We recommend Ref. 9 as a good source for this topic. Topological classification of equilibria is found in Refs. 10–12.

PERIODIC STATE AND ITS STABILITY

Periodic state plays the central role in nonlinear circuit dynamics. A basic tool for studying periodic state and its related property is the Poincaré map by which a continuous time dynamical system reduces to a discrete time dynamical system. A periodic state is then transformed to a fixed point of the Poincaré map. Hence a similar argument to equilibria will be developed for fixed points.

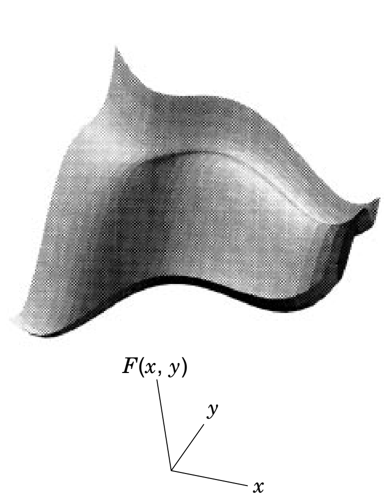

Figure 14. Surface of the dissipative function, Eq. (47). Each stationary point corresponds to the equilibrium point in Fig. 13.

Periodic State of Autonomous Systems

Consider an autonomous system

$$\dot{\mathbf{x}} = \mathbf{f}(\mathbf{x}, \lambda), \qquad \mathbf{x} \in \mathbf{R}^n, \lambda \in \mathbf{R}^m \tag{95}$$

where $\mathbf{x} \in \mathbf{R}^n$ is a state vector and $\lambda \in \mathbf{R}^m$ is a system parameter. Suppose that Eq. (95) have a periodic solution $\varphi(t, \mathbf{x}_0, \lambda)$ with period L. The orbit

$$C = Orb(\mathbf{x}_0) = \{\mathbf{x} \in \mathbf{R}^n \mid \mathbf{x} = \varphi(t, \mathbf{x}_0, \lambda), t \in [0, L]\} \tag{96}$$

forms a closed curve in the state space $\mathbf{R}^n$. This is an invariant set of Eq. (95). That is,

$$\varphi(t, C, \lambda) = C \tag{97}$$

A small perturbation or variation $\xi(t)$ from the periodic solution obeys the following variational equation:

$$\dot{\xi}(t) = \mathbf{A}(t)\xi(t) \tag{98}$$

where

$$\mathbf{A}(t) = D\mathbf{f}(\varphi(t, \mathbf{x}_0, \lambda), \lambda) = \frac{\partial \mathbf{f}}{\partial \mathbf{x}}(\varphi(t, \mathbf{x}_0, \lambda), \lambda) \tag{99}$$

is the Jacobian matrix with respect to $\mathbf{x}$. By the periodicity of $\varphi(t, \mathbf{x}_0, \lambda)$, the matrix $\mathbf{A}(t)$ becomes a periodic matrix with the same period L:

$$\mathbf{A}(t) = \mathbf{A}(t + L), \qquad t \in \mathbf{R} \tag{100}$$

Hence Eq. (98) is a linear equation with periodic coefficients. Similar to the hyperbolic equilibrium point, we can discuss the hyperbolicity of periodic solution. We will study this by example.

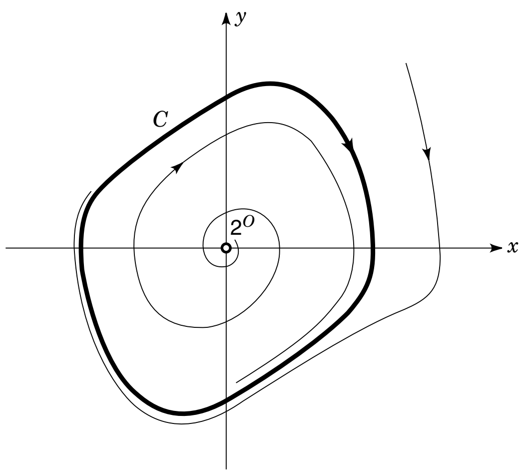

Figure 16. Phase portrait of the van der Pol equation, Eq. (89), with ϵ = 0.5 and γ = 1. The closed curve C indicates a stable limit cycle.

Example 6. 1. *Self-excited oscillation.* Consider the van der Pol equation [Eq. (89)] in Example 5(2). Figure 16 shows the phase portrait of Eq. (89) with $\epsilon = 0.5$, $\gamma = 1.0$. We see that the origin is a source and a closed curve C which is the ω limit set of any point in the phase plane except the origin. The closed curve C is the orbit of the periodic solution with an initial state in C. As we will see later, the periodic solution is orbitally stable. In a two-dimensional autonomous system, an isolated closed orbit is called a *limit cycle.* Thus the van der Pol equation has a unique stable limit cycle. This corresponds to a self-excited oscillatory phenomenon in circuit dynamics. Note that we could not solve Eq. (89) explicitly so that an appropriate numerical algorithm, such as the fourth-order Runge–Kutta method, is used to accomplish the phase portrait.

2. *Hard oscillation.* Consider the equation

$$\begin{aligned} \dot{x} &= y \\ \dot{y} &= -x - \epsilon(1 - \beta x^2 + x^4)y \end{aligned} \tag{101}$$

Equation (101) is the van der Pol equation with a hard characteristic. That is, the nonlinear characteristic is assumed to be a fifth-order polynomial. Figure 17 shows the phase portrait for $\epsilon = 0.2$, $\beta = 3.5$. Two limit cycles C_1 and C_2, one of which is stable and another unstable, exist and the origin is a sink $_0O$ in this case. Hence we have two attractors: a stable limit cycle C_1 and a stable equilibrium point $_0O$. The basin of the latter equilibrium point is the region surrounded by the unstable limit cycle cycle C_2. The outer region of the unstable limit cycle C_2 is then the basin of the stable limit cycle C_1. According to the initial state we specify, the final steady state becomes the sink $_0O$ or the stable limit cycle C_1. This shows an example of the existence of multistable states. In the circuit, if the initial state is small, then the oscillatory state is never realized. To observe an oscillatory state corresponding to the stable limit cycle we must give an initial state large enough to enter the basin of the limit cycle C_1. This oscillatory process is called a *hard oscillation.* On the other hand, the process stated in Example 6, item 1, is called a *soft oscillation.*

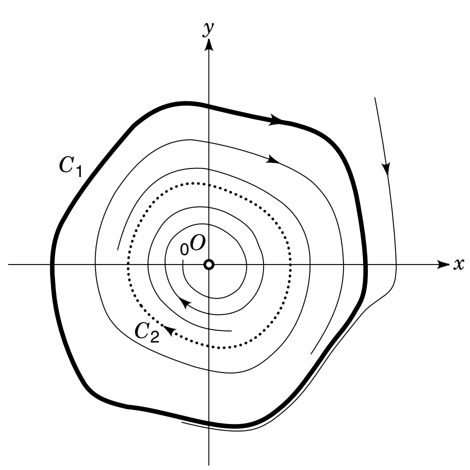

Figure 17. Phase portrait of a hard oscillator equation, Eq. (101), with ϵ = 0.2 and β = 3.5. Closed curves C_1 and C_2 indicate a stable and an unstable limit cycle, respectively.

Poincaré Map for Autonomous Systems

The definition of a Poincaré map, or first return map, for a periodic solution is quite simple. Suppose that Eq. (95) has a periodic solution $\varphi(t, \mathbf{x}_0, \lambda)$ through the point $\mathbf{x}_0$. We choose a hypersurface $\Pi \subset \mathbf{R}^n$ to intersect transversally the periodic orbit at $\mathbf{x}_0$, Then for each point $\mathbf{x}_1 \in \Pi$ sufficiently near $\mathbf{x}_0$, the solution through $\mathbf{x}_1$ will return to Π again at a point $\mathbf{x}_2 \in \Pi$ near $\mathbf{x}_0$ (see Fig. 18). The mapping $\mathbf{x}_1 \mapsto \mathbf{x}_2$ is called the Poincaré map T. That is, T is defined as

$$T: \qquad \Pi \to \Pi; \quad \mathbf{x}_1 \mapsto \mathbf{x}_2 = T(\mathbf{x}_1) = \varphi(\tau, \mathbf{x}_1, \lambda) \tag{102}$$

where τ is the return time and depends on the initial point $\mathbf{x}_1$. The hypersurface Π is locally defined and is called a local cross section or a Poincaré section. Assume that Π is described as

$$\Pi = \{\mathbf{x} \in \mathbf{R}^n \mid q(\mathbf{x}) = 0\} \tag{103}$$

where q is a scalar function from $\mathbf{R}^n$ to $\mathbf{R}$. The transversality condition is then expressed by

$$\frac{\partial q(\mathbf{x}_0)}{\partial \mathbf{x}}\mathbf{f}(\mathbf{x}_0, \lambda) = \mathbf{f}(\mathbf{x}_0, \lambda) \cdot grad\, q(\mathbf{x}_0) \neq 0 \tag{104}$$

Note that dim $\Pi = n - 1$. Once the Poincaré map T is defined, we have a recurrent formula or difference equation of the

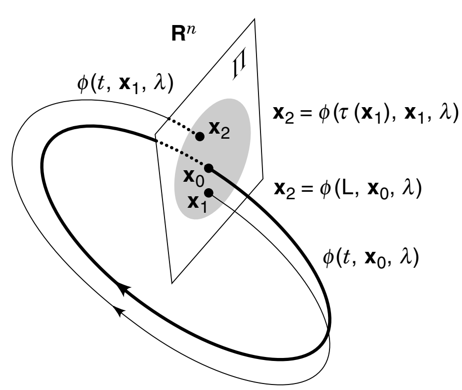

Figure 18. Periodic orbit and Poincaré map. Local cross section is the hypersurface Π.

form

$$\mathbf{x}_{k+1} = T(\mathbf{x}_k), \quad \mathbf{x}_k \in \Pi, \qquad k = 1, 2, \ldots \tag{105}$$

By the uniqueness theorem of differential equations the map T has a unique inverse map T^{-1}. Moreover, if the vector field (95) is differentiable, T and T^{-1} is also differentiable; that is, T is a diffeomorphism on Π near $\mathbf{x}_0$. Because $\mathbf{x}_0$ is on the periodic orbit, we have

$$T(\mathbf{x}_0) = \mathbf{x}_0 \tag{106}$$

That is, $\mathbf{x}_0$ is a fixed point of T. If L is the period of the periodic solution, then the return time becomes $\tau(\mathbf{x}_0) = L$.

Stroboscopic Mapping: Poincaré Map for Periodic Nonautonomous Systems

Consider a nonautonomous system

$$\dot{\mathbf{x}} = \mathbf{f}(t, \mathbf{x}, \lambda), \mathbf{x} \in \mathbf{R}^n, \lambda \in \mathbf{R}^m \tag{107}$$

where $\mathbf{x} \in \mathbf{R}^n$ is a state vector and $\lambda \in \mathbf{R}^m$ is a system parameter. We assume that $\mathbf{f}$ is periodic in t with period 2π:

$$\mathbf{f}(t, \mathbf{x}, \lambda) = \mathbf{f}(t + 2\pi, \mathbf{x}, \lambda) \tag{108}$$

for all $t \in \mathbf{R}$. Equation (107) describes a class of dynamic nonlinear circuits with a periodic forcing term. A nonlinear circuit with an ac operation is a typical example of this class. Without loss of generality, we assume that the period of the external forcing is 2π. Suppose that Eq. (107) has a solution $\mathbf{x}(t) = \varphi(t, \mathbf{x}_0, \lambda)$ with $\mathbf{x}(0) = \varphi(0, \mathbf{x}_0, \lambda) = \mathbf{x}_0$. This time we have the periodic property equation, Eq. (108). Hence for every 2π instance the vector field equation, Eq. (107), returns the same value so that a stroboscopic sampling of the solution can be achieved under the fixed vector field. That is, we can define the stroboscopic mapping as the Poincaré map (see Fig. 19):

$$T: \qquad \mathbf{R}^n \to \mathbf{R}^n; \quad \mathbf{x}_0 \mapsto \mathbf{x}_1 = T(\mathbf{x}_0) = \varphi(2\pi, \mathbf{x}_0, \lambda) \tag{109}$$

If a solution $\mathbf{x}(t) = \varphi(t, \mathbf{x}_0, \lambda)$ is periodic with period 2π, then the intial state $\mathbf{x}_0$ is a fixed point of T:

$$T(\mathbf{x}_0) = \mathbf{x}_0 \tag{110}$$

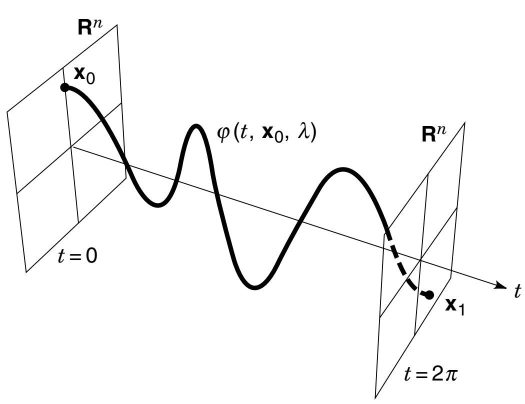

Figure 19. Stroboscopic mapping. Poincaré map for a periodic nonautonomous system.

If $\mathbf{x}(t)$ is a periodic solution with period $2k\pi$, then the point $\mathbf{x}_0$ is a periodic point of T with period k such that $T^k(\mathbf{x}_0) = \mathbf{x}_0$ and $T^j(\mathbf{x}_0) \neq \mathbf{x}_0$ for $j = 1, 2, \ldots, k-1$. Hence there are always k points $\mathbf{x}_0$, $\mathbf{x}_1 = T(\mathbf{x}_0), \ldots, \mathbf{x}_{k-1} = T^{k-1}(\mathbf{x}_0)$ which are all fixed points of T^k. Thus the behavior of periodic solution of Eq. (107) is reduced to the behavior of fixed or periodic points of the map T.

Hyperbolic Fixed Point and Its Stability

Now we consider the qualitative property of a fixed point of the Poincaré map T. In the following for the notational convenience we consider T defined by Eq. (109). The same discussion is applied to Eq. (102). Suppose that $\mathbf{x}_0 \in \mathbf{R}^n$ is a fixed of T. The characteristic equation of the fixed point $\mathbf{x}_0$ is defined by

$$\chi(\mu) = \det(\mu\mathbf{I}_n - DT(\mathbf{x}_0)) = 0 \tag{111}$$

where $DT(\mathbf{x}_0)) = \partial T(\mathbf{x}_0)/\partial \mathbf{x}_0$ denotes the derivative of T. Near $\mathbf{x}_0$ the map T is approximated by its derivative $DT(\mathbf{x}_0)$. This is indeed possible if the fixed point is hyperbolic. Here we call $\mathbf{x}_0$ a hyperbolic fixed point of T, if $DT(\mathbf{x}_0)$ is hyperbolic, that is, all the absolute values of the eigenvalues of $DT(\mathbf{x}_0)$ are different from unity. Let $\mathbf{x}_0$ be a hyperbolic fixed point of T and let $\mathbf{E}^u$ be the intersection of $\mathbf{R}^n$ and the direct sum of generalized eigenspace of $DT(\mathbf{x}_0)$ corresponding to the eigenvalues μ_i such that $|\mu_i| > 1$. Similarly, let $\mathbf{E}^s$ be the intersection of $\mathbf{R}^n$ and the direct sum of generalized eigenspace of $DT(\mathbf{x}_0)$ corresponding to the eigenvalues μ_i such that $|\mu_i| < 1$. $\mathbf{E}^u$ or $\mathbf{E}^s$ is called the unstable or stable subspace of $DT(\mathbf{x}_0)$. The map version of the Hartman–Grobman theorem shows that $\mathbf{E}^u$ and $\mathbf{E}^s$ have the following properties:

$$\begin{aligned}&\text{(a) } \mathbf{R}^n = \mathbf{E}^u \oplus \mathbf{E}^s, \qquad DT(\mathbf{E}^u) = \mathbf{E}^u, \qquad DT(\mathbf{E}^s) = \mathbf{E}^s \\ &\text{(b) } \dim \mathbf{E}^u = \#\{\mu_i \mid |\mu_i| > 1\}, \qquad \dim \mathbf{E}^s = \#\{\mu_i \mid |\mu_i| < 1\}\end{aligned} \tag{112}$$

Let $L^u = DT(\mathbf{x}_0)|_{\mathbf{E}^u}$ and $L^s = DT(\mathbf{x}_0)|_{\mathbf{E}^s})$. Then the topological type of a hyperbolic fixed point is determined by (1) the dim $\mathbf{E}^u$ (or dim $\mathbf{E}^s$) and (2) the orientation preserving or reversing property of L^u (or L^s). The latter condition is equivalent to the positive or negative sign of det L^u (or det L^s) and is the additional condition comparing with a hyperbolic equilibrium point. We refer a hyperbolic fixed point with det $L^u > 0$ to a direct type (i.e., D-type) and refer a hyperbolic fixed point with det $L^u < 0$ to an inverse type (i.e., I-type). Note that $DT(\mathbf{x}_0)$ is an orientation preserving map, that is, det $DT(\mathbf{x}_0) > 0$. Combining the dimensionality, we have $2n$ topologically different types of hyperbolic fixed points. These types are

$$\{{}_0D,\ {}_1D, \ldots,\ {}_nD;\ {}_1I,\ {}_2I, \ldots,\ {}_{n-1}I\} \tag{113}$$

where D and I denote the type of the fixed point and the subscript integer indicates the dimension of the unstable subspace: $k = \dim \mathbf{E}^u$. Usually a completely stable fixed point ${}_0D$ is called a *sink,* a completely unstable fixed point ${}_nD$ is called a *source,* and others are called *saddles.*

Remark 5. 1. The classification stated above is also obtained from the distribution of the eigenvalues, also called the characteristic multipliers, of Eq. (111). That is, D and I correspond to the even and odd number of characteristic multipliers on the real axis $(-\infty, -1)$, and k indicates the number of characteristic multipliers outside the unit circle in the complex plane. The distribution can be checked by the coefficients of Eq. (111).

2. The derivative $DT(\mathbf{x}_0) = \partial T(\mathbf{x}_0)/\partial \mathbf{x}$ is obtained from the solution of the variational equation with respect to the initial state of the periodic solution $\mathbf{x}(t) = \varphi(t, \mathbf{x}_0, \lambda)$ with $\mathbf{x}(0) = \varphi(0, \mathbf{x}_0, \lambda) = \mathbf{x}_0$. Consider the nonautonomous case, Eq. (107). We have the identity relation:

$$\begin{aligned} &\dot{\varphi}(t, \mathbf{x}_0, \lambda) = \mathbf{f}(t, \varphi(t, \mathbf{x}_0, \lambda), \lambda) \\ &\varphi(0, \mathbf{x}_0, \lambda) = \mathbf{x}_0 \end{aligned} \tag{114}$$

Differentiating these relations with respect to the initial state, we have

$$\begin{aligned} &\frac{d}{dt}\frac{\partial \varphi(t, \mathbf{x}_0, \lambda)}{\partial \mathbf{x}_0} = \frac{\partial \mathbf{f}(t, \varphi(t, \mathbf{x}_0, \lambda), \lambda)}{\partial \mathbf{x}}\frac{\partial \varphi(t, \mathbf{x}_0, \lambda)}{\partial \mathbf{x}_0} \\ &\frac{\partial \varphi(0, \mathbf{x}_0, \lambda)}{\partial \mathbf{x}_0} = \mathbf{I}_n \end{aligned} \tag{115}$$

This is the matrix version of the variational equation with respect to the initial state. We call the solution the *principal fundamental matrix solution* and write

$$\Phi(t) = \frac{\partial \varphi(t, \mathbf{x}_0, \lambda)}{\partial \mathbf{x}_0}, \qquad \Phi(0) = \mathbf{I}_n \tag{116}$$

From the definition of the Poincaré map, we obtain

$$DT(\mathbf{x}_0) = \frac{\partial T(\mathbf{x}_0)}{\partial \mathbf{x}_0} = \frac{\partial \varphi(2\pi, \mathbf{x}_0, \lambda)}{\partial \mathbf{x}_0} = \Phi(2\pi) \tag{117}$$

From Liouville's theorem we have

$$\begin{aligned} \det DT(\mathbf{x}_0) &= \det\Phi(2\pi) \\ &= \det\Phi(0)\exp \\ &\quad \left\{\int_0^L trace\left(\frac{\partial \mathbf{f}(\tau, \varphi(\tau, \mathbf{x}_0, \lambda), \lambda)}{\partial \mathbf{x}}\right)d\tau\right\} \\ &= \exp\left\{\int_0^L trace\left(\frac{\partial \mathbf{f}(\tau, \varphi(\tau, \mathbf{x}_0, \lambda), \lambda)}{\partial \mathbf{x}}\right)d\tau\right\} > 0 \end{aligned} \tag{118}$$

Thus T is an orientation preserving diffeomorphism.

3. In an autonomous system, Eq. (95), a periodic solution always has at least one characteristic multiplier that is equal to unity. Indeed, a periodic solution satisfies the relation

$$\dot{\varphi}(t, \mathbf{x}_0, \lambda) = \mathbf{f}(\varphi(t, \mathbf{x}_0, \lambda), \lambda) \tag{119}$$

Differentiating by t yields

$$\ddot{\varphi}(t, \mathbf{x}_0, \lambda) = \frac{\partial \mathbf{f}(\varphi(t, \mathbf{x}_0, \lambda), \lambda)}{\partial \mathbf{x}}\dot{\varphi}(t, \mathbf{x}_0, \lambda) = \mathbf{A}(t)\dot{\varphi}(t, \mathbf{x}_0, \lambda) \tag{120}$$

Hence $\dot{\varphi}(t, \mathbf{x}_0, \lambda)$ is a solution of the variational equation, Eq. (98). Let the principal fundamental matrix solution be $\Phi(t)$, then $\dot{\varphi}(t, \mathbf{x}_0, \lambda)$ is expressed by

$$\dot{\varphi}(t, \mathbf{x}_0, \lambda) = \Phi(t)\dot{\varphi}(0, \mathbf{x}_0, \lambda) \tag{121}$$

Hence, using Eq. (121) and the periodicity of the solution, we have

$$\dot{\varphi}(L, \mathbf{x}_0, \lambda) = \Phi(L)\dot{\varphi}(0, \mathbf{x}_0, \lambda) = \dot{\varphi}(0, \mathbf{x}_0, \lambda) \tag{122}$$

This means that $\Phi(L)$ has the unity multiplier with the eigenvector:

$$\dot{\varphi}(0, \mathbf{x}_0, \lambda) = \mathbf{f}(\mathbf{x}_0, \lambda) \tag{123}$$

From this property the derivative of the Poincaré map defined by Eq. (102) has at least one unity multiplier.

4. *Stable and unstable manifolds of a hyperbolic fixed point.* The subsets leaving from and approaching a hyperbolic fixed point $\mathbf{x}_0$ are called the *unstable manifold,* $W^s(\mathbf{x}_0)$, and the *stable manifold,* $W^u(\mathbf{x}_0)$, respectively. They are defined as

$$\begin{aligned} W^u(\mathbf{x}_0) &= \{\mathbf{u} \in \mathbf{R}^n \mid \lim_{k\to-\infty} T^k(\mathbf{u}) = \mathbf{x}_0\} \\ W^s(\mathbf{x}_0) &= \{\mathbf{u} \in \mathbf{R}^n \mid \lim_{k\to\infty} T^k(\mathbf{u}) = \mathbf{x}_0\} \end{aligned} \tag{124}$$

$\mathbf{E}^u$ and $\mathbf{E}^s$ defined in Eq. (112) are tangent spaces to $W^u(\mathbf{x}_0)$ and $W^s(\mathbf{x}_0)$ at $\mathbf{x}_0$, and

$$\begin{aligned} &\dim \mathbf{E}^u = \dim W^u(\mathbf{x}_0), \\ &\dim \mathbf{E}^s = \dim W^s(\mathbf{x}_0), \\ &W^u(\mathbf{x}_0) \cap W^s(\mathbf{x}_0) = \mathbf{x}_0 \end{aligned} \tag{125}$$

Thus stable and unstable manifolds have global information of the phase portrait of the Poincaré map T. In the two-dimensional case a ${}_1D$ or ${}_1I$ fixed point has a stable invariant curve and an unstable invariant curve, which are also called ω branch and α branch of the fixed point, respectively.

5. *Phase portrait for the Poincaré map, Eq. (109).* Similar to the phase portrait of an autonomous system, we can define the phase portrait of the Poincaré map. Suppose that a discrete time dynamical system is defined by Eq. (109). We define the point set, called the *orbit,* through $\mathbf{x}_0$:

$$Orb(\mathbf{x}_0) = \{\mathbf{x}_k \in \mathbf{R}^n \mid \mathbf{x}_k = T^k(\mathbf{x}_0),\ k = \cdots, -1, 0, 1, \cdots\} \tag{126}$$

A fixed point $\mathbf{x}_0 = T(\mathbf{x}_0)$ has a single-point orbit $Orb(\mathbf{x}_0) = \{\mathbf{x}_0\}$. Similarly, a k-periodic point $\mathbf{x}_0 = T^k(\mathbf{x}_0)$ has the orbit $Orb(\mathbf{x}_0) = \{\mathbf{x}_0, \mathbf{x}_1, \cdots, \mathbf{x}_{k-1}\}$. An orbit is an invariant set in $\mathbf{R}^n$:

$$T(Orb(\mathbf{x}_0)) = Orb(\mathbf{x}_0) \tag{127}$$

The stable and unstable manifolds defined by Eq. (124) are other examples of an invariant set of T. A phase portrait of the Poincaré map T is then the set of all orbits in the phase space $\mathbf{R}^n$. We illustrate schematically some typical orbits and invariant sets to show the global structure of the phase space.

6. *Numerical computation of hyperbolic fixed point.* A hyperbolic fixed point can be found by Newton's method as follows. Let Eq. (110) be the form

$$\mathbf{F}(\mathbf{x}) = \mathbf{x} - T(\mathbf{x}) = 0 \tag{128}$$

Then from Eq. (117) the Jacobian matrix becomes

$$D\mathbf{F}(\mathbf{x}) = \mathbf{I}_n - DT(\mathbf{x}) = \mathbf{I}_n - \Phi(2\pi) \tag{129}$$

This matrix is nonsingular if a fixed point is hyperbolic. Hence Newton's iteration

$$\begin{aligned} \mathbf{x}^{(k+1)} &= \mathbf{x}^{(k)} + \mathbf{h}, \qquad k = 0, 1, 2, \cdots \\ D\mathbf{F}(\mathbf{x}^{(k)})\mathbf{h} &= -\mathbf{F}(\mathbf{x}^{(k)}) \end{aligned} \tag{130}$$

works well from an appropriate initial guess $\mathbf{x}^{(0)}$.

Example 7. 1. *Two-dimensional hyperbolic fixed points.* We have four different types of hyperbolic fixed points: ${}_0D$, ${}_1D$, ${}_1I$, ${}_2D$; they are called a completely stable, a directly unstable, an inversely unstable, and a completely unstable fixed point, respectively. They are obtained under the following conditions. Let Eq. (111) be given by

$$\chi(\mu) = \det[\mu \mathbf{I}_2 - DT(\mathbf{x}_0, \lambda)] = \mu^2 + a_1\mu + a_2 = 0 \tag{131}$$

Then we have:

(a) If $0 < a_2 < 1$, $0 < \chi(-1)$, $0 < \chi(1)$, then the hyperbolic fixed point is ${}_0D$,
(b) If $0 < a_2$, $0 < \chi(-1)$, then the hyperbolic fixed point is ${}_1D$,
(c) If $0 < a_2$, $0 < \chi(1)$, then the hyperbolic fixed point is ${}_1I$,
(d) If $1 < a_2$, $0 < \chi(-1)$, $0 < \chi(1)$, then the hyperbolic fixed point is ${}_2D$.

These relations are illustrated in Fig. 20.

2. *Periodic solutions of Duffing's equation.* Consider the following Duffing's equation [cf. Eq. (20)]:

$$\begin{aligned} \dot{x} &= y \\ \dot{y} &= -0.1y - x^3 + 0.3\cos t \end{aligned} \tag{132}$$

Figure 21 shows the phase portrait of the Poincaré map T. Equation (132) has three periodic solutions: a nonresonant solution S_1, a resonant solution S_2, and an unstable solution ${}_1D$. The former two solutions are sinks, and the latter a directly unstable saddle. These periodic trajectories are shown by closed dotted curves. Two curves indicated α and ω show the unstable invariant curve $W^u({}_1D)$ and the stable invariant curves $W^s({}_1D)$ of the saddle fixed point ${}_1D$. The ω branch is the boundary curve of two basins of the attractors S_1 and S_2. By the numerical computation in Remark 5(6), the location (x, y) of the three fixed points is found to be $S_1(-0.3228, 0.0360)$, $S_2(1.1381, 0.7446)$, and ${}_1D(-0.9170, 0.3812)$.

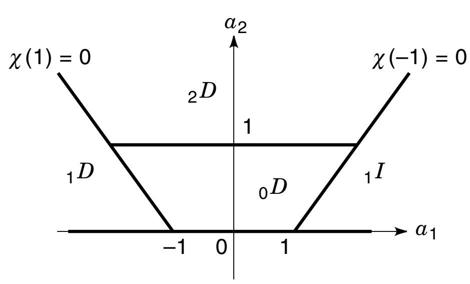

Figure 20. Topological classification of fixed points: two-dimensional case.

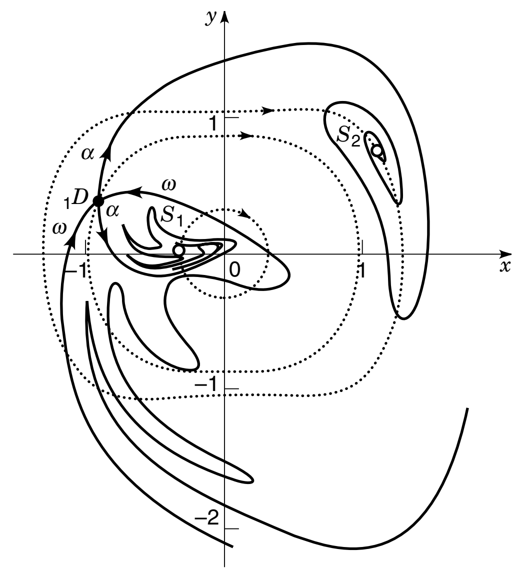

Figure 21. Phase portrait of the Poincaré map defined by Eq. (132). Closed dotted curves indicate periodic solutions.

Harmonic Resonance in Duffing's Equation

Nonlinear resonance occurs typically in Duffing's equation. The simplest resonant phenomenon is a harmonic resonance. It is observed when the frequency of a free harmonic oscillator is nearly equal to that of an injected external periodic signal. In the following we will discuss this phenomenon by using an analytical approach: the perturbation method and the averaging method.

Perturbation Method. Let us consider the periodic solution of Duffing's equation:

$$\ddot{x} + \epsilon\zeta\dot{x} + \Omega^2 x + \epsilon c x^3 = B\cos t \tag{133}$$

where ϵ is a small parameter. Rewriting this equation as

$$\ddot{x} + \Omega^2 x = B\cos t - \epsilon(\zeta\dot{x} + cx^3) \tag{134}$$

we see that Eq. (133) is a quasilinear system. Hence we will find periodic solutions by the standard perturbation method. Assume that a periodic solution is expressed in the formal power series of ϵ as

$$x(t) = x_0(t) + \epsilon x_1(t) + \epsilon^2 x_2(t) + \epsilon^3 x_3(t) + \cdots \tag{135}$$

Substituting Eq. (135) into Eq. (134) and equating the same power of ϵ, we have

$$\begin{aligned} \epsilon^0: &\quad \ddot{x}_0 + \Omega^2 x_0 = B\cos t \\ \epsilon^1: &\quad \ddot{x}_1 + \Omega^2 x_1 = -\zeta\dot{x}_0 - cx_0^3 \\ \epsilon^2: &\quad \ddot{x}_2 + \Omega^2 x_2 = -3cx_0^2 x_1 - \zeta\dot{x}_1 \end{aligned} \tag{136}$$

From perturbation theory, if Eq. (136) has an isolated periodic solution, then for sufficiently small ϵ there exists the periodic solution in Eq. (134). Hence to find the periodic solution we will consider two cases: a nonresonant case and a resonant case, separately.

Nonresonant Case Where $\Omega \neq 1$. Solving Eq. (136) consecutively, we have

$$x_0(t) = \frac{B}{\Omega^2 - 1}\cos t$$
$$x_1(t) = \frac{B\zeta}{(\Omega^2-1)^2}\sin t - \frac{3cB^3}{4(\Omega^2-1)^4}\cos t - \frac{cB^3}{4(\Omega^2-1)^3(\Omega^2-9)}\cos 3t \tag{137}$$

Thus for the nonresonant case we have a unique periodic state in the form of Eq. (135).

Resonant Case Where $\Omega \cong 1$. As $\Omega \cong 1$, we put

$$1 - \Omega^2 = \epsilon a, \qquad B = \epsilon b \tag{138}$$

Note that a indicates a measure of the frequency difference between free and external frequencies. Hence the resonant case Eq. (134) becomes

$$\ddot{x} + x = \epsilon(b\cos t + ax - \zeta\dot{x} - cx^3) \tag{139}$$

Now we will try to find the periodic solution in the form of Eq. (135). Substituting Eq. (135) into Eq. (139), we find

$$\begin{aligned} \epsilon^0 &: \ddot{x}_0 + x_0 = 0 \\ \epsilon^1 &: \ddot{x}_1 + x_1 = b\cos t + ax_0 - \zeta\dot{x}_0 - cx_0^3 \\ &\cdots \end{aligned} \tag{140}$$

By solving the first equation of Eq. (140), we have

$$x_0(t) = M_0\cos t + N_0\sin t \tag{141}$$

where M_0 and N_0 are unknown coefficients. They are determined as follows: Substituting Eq. (141) into the second equation of Eq. (140), we have

$$\begin{aligned} \ddot{x}_1 + x_1 = &\left\{\zeta M_0 + \left(a - \frac{3}{4}cr^2\right)N_0\right\}\sin t \\ &+ \left\{\left(a - \frac{3}{4}cr^2\right)M_0 - \zeta N_0 + b\right\}\cos t \\ &+ \frac{1}{4}c(N_0^2 - 3M_0^2)N_0\sin 3t \\ &+ \frac{1}{4}c(3N_0^2 - M_0^2)M_0\cos 3t \end{aligned} \tag{142}$$

where $r^2 = M_0^2 + N_0^2$. Equation (142) has a periodic solution if and only if the following conditions are satisfied:

$$\begin{aligned} P(M_0, N_0) &= \zeta M_0 + \left(a - \frac{3}{4}cr^2\right)N_0 = 0 \\ Q(M_0, N_0) &= \left(a - \frac{3}{4}cr^2\right)M_0 - \zeta N_0 + b = 0 \end{aligned} \tag{143}$$

When a solution (M_0, N_0) of Eq. (143) is an isolate root, i.e., the Jacobian matrix:

$$\begin{bmatrix} \dfrac{\partial P}{\partial M_0} & \dfrac{\partial P}{\partial N_0} \\ \dfrac{\partial Q}{\partial M_0} & \dfrac{\partial Q}{\partial N_0} \end{bmatrix} \tag{144}$$

is nonsingular at this root, then Eq. (142) has a periodic solution

$$\begin{aligned} x_1(t) = &M_1\cos t + N_1\sin t \\ &- \frac{1}{32}c(N_0^2 - 3M_0^2)N_0\sin 3t \\ &- \frac{1}{32}c(3N_0^2 - M_0^2)M_0\cos 3t \end{aligned} \tag{145}$$

where M_1 and N_1 are still unknown coefficients. Thus Eq. (143) determines the first term of Eq. (135), called the generating solution of the first equation of Eq. (140). Although higher-order terms of ϵ of Eq. (135) have little effect on this solution, the generating solution (i.e., the zeroth order approximate solution) determines the behavior of the periodic solution, Eq. (135). From Eq. (143) we find the relation

$$\left\{\left(a - \frac{3}{4}cr^2\right)^2 + \zeta^2\right\}r^2 = b^2 \tag{146}$$

This simple relation gives then the amplitude relationship or frequency relationship of the harmonic resonance. Figure 22 shows an amplitude characteristic of Eq. (146)—that is, the relationship between b and r—in the case where $a = c = 1.0$. Also plotted in Fig. 23 is a frequency response of the harmonic oscillation—that is, the relationship between a and r in the case where $c = 1.0$ and $\zeta = 0.2$. Thus we see that there are three kinds of periodic solutions under certain values of b, a, and r. We will return these characteristics after the discussion of their stability.

Stability Analysis. After finding a periodic solution of the form Eq. (135), we will study the stability of the periodic solution. Let the periodic solution be

$$x(t) = x_0(t) + \epsilon x_1(t) + \epsilon^2 x_2(t) + \epsilon^3 x_3(t) + \cdots = \varphi^*(t) \tag{147}$$

For a small variation

$$x(t) = \varphi^*(t) + \xi(t) \tag{148}$$

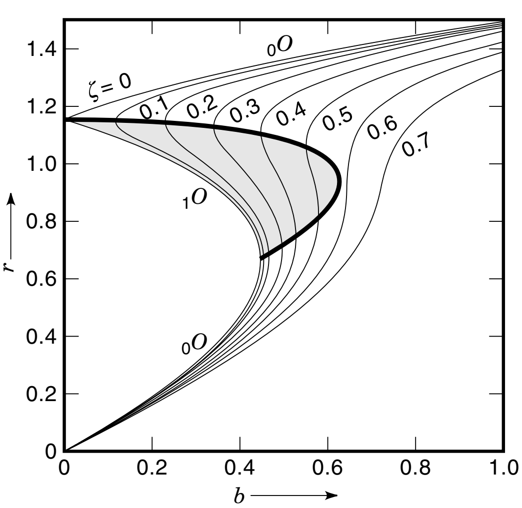

Figure 22. Amplitude characteristic curves of Eq. (146).

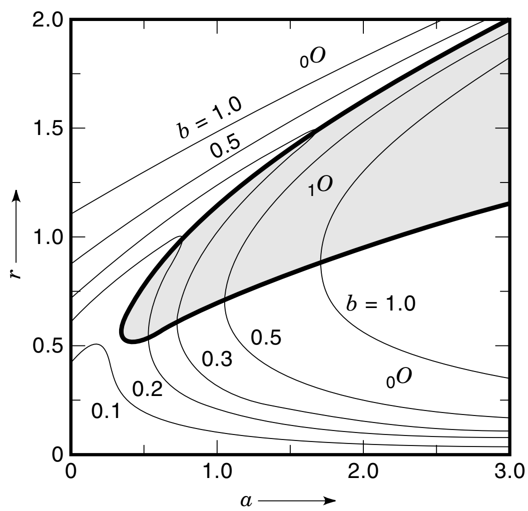

Figure 23. Frequency characteristic curves of Eq. (146).

the variational equation becomes

$$\ddot{\xi} + \xi = -\epsilon\{3c(\varphi^*(t))^2\xi + \zeta\dot{\xi}\} \tag{149}$$

Hence we calculate the fundamental solutions of Eq. (149), that is, the solutions

$$\begin{aligned} \xi^{(1)}(t) &= \xi_0^{(1)}(t) + \epsilon\xi_1^{(1)}(t) + \epsilon^2\xi_2^{(1)}(t) + \cdots \\ \xi^{(2)}(t) &= \xi_0^{(2)}(t) + \epsilon\xi_1^{(2)}(t) + \epsilon^2\xi_2^{(2)}(t) + \cdots \end{aligned} \tag{150}$$

with the initial conditions

$$\begin{aligned} &\xi_0^{(1)}(0) = 1, \quad \dot{\xi}_0^{(1)}(0) = 0, \quad \xi_k^{(1)}(0) = \dot{\xi}_k^{(1)}(0) = 0 \\ &\xi_0^{(2)}(0) = 0, \quad \dot{\xi}_0^{(2)}(0) = 1, \quad \xi_k^{(2)}(0) = \dot{\xi}_k^{(2)}(0) = 0 \quad (k = 1, 2, \ldots) \end{aligned} \tag{151}$$

Substituting Eq. (150) into Eq. (149) and equating the same power of ϵ, we have

$$\begin{aligned} &\ddot{\xi}_0^{(1)} + \xi_0^{(1)} = 0 \\ &\ddot{\xi}_0^{(2)} + \xi_0^{(2)} = 0 \\ &\ddot{\xi}_1^{(1)} + \xi_1^{(1)} = -\epsilon\{3c(\varphi^*(t))^2\xi_0^{(1)} + \zeta\dot{\xi}_0^{(1)}\} \\ &\ddot{\xi}_1^{(2)} + \xi_1^{(2)} = -\epsilon\{3c(\varphi^*(t))^2\xi_0^{(2)} + \zeta\dot{\xi}_0^{(2)}\} \end{aligned} \tag{152}$$

Hence the solutions of Eq. (152) can be found as

$$\begin{aligned} &\xi_0^{(1)} = \cos t, \qquad \xi_0^{(2)} = \sin t \\ &\xi_1^{(1)}(t) = \int_0^t \left[-3c(\varphi^*(\tau))^2\cos\tau + \zeta\sin\tau\right]\sin(t-\tau)d\tau \\ &\xi_1^{(2)}(t) = \int_0^t \left[-3c(\varphi^*(\tau))^2\sin\tau - \zeta\cos\tau\right]\sin(t-\tau)d\tau \end{aligned} \tag{153}$$

The characteristic equation is given by

$$\chi(\mu) = \begin{vmatrix} \mu - \xi^{(1)}(2\pi) & -\xi^{(2)}(2\pi) \\ -\dot{\xi}^{(1)}(2\pi) & \mu - \dot{\xi}^{(2)}(2\pi) \end{vmatrix} = \mu^2 + a_1\mu + a_2 = 0 \tag{154}$$

where

$$\begin{aligned} a_1 &= -\{\xi^{(1)}(2\pi) + \dot{\xi}^{(2)}(2\pi)\} = -2 - \epsilon\{\xi_1^{(1)}(2\pi) + \dot{\xi}_1^{(2)}(2\pi)\} \\ &\quad - \epsilon^2\{\xi_2^{(1)}(2\pi) + \dot{\xi}_2^{(2)}(2\pi)\} - \cdots \\ a_2 &= \xi^{(1)}(2\pi)\dot{\xi}^{(2)}(2\pi) - \xi^{(2)}(2\pi)\dot{\xi}^{(1)}(2\pi) \\ &= 1 + \epsilon\{\xi_1^{(1)}(2\pi) + \dot{\xi}_1^{(2)}(2\pi)\} \\ &\quad + \epsilon^2\{\xi_2^{(1)}(2\pi) + \dot{\xi}_2^{(2)}(2\pi) + \xi_1^{(1)}(2\pi)\dot{\xi}_1^{(2)}(2\pi) \\ &\quad - \xi_1^{(2)}(2\pi)\dot{\xi}_1^{(1)}(2\pi)\} + \cdots \end{aligned} \tag{155}$$

Hence the conditions stated in Example 7(1) become

$$\begin{aligned} \chi(-1) &= 1 - a_1 + a_2 = 4 + \epsilon\{\cdots\} + \cdots > 0 \\ \chi(1) &= 1 + a_1 + a_2 \\ &= \epsilon^2\{\xi_1^{(1)}(2\pi)\dot{\xi}_1^{(2)}(2\pi) - \xi_1^{(2)}(2\pi)\dot{\xi}_1^{(1)}(2\pi)\} + \epsilon^3\{\cdots\} + \cdots \\ a_2 &= 1 + \epsilon\{\xi_1^{(1)}(2\pi) + \dot{\xi}_1^{(2)}(2\pi)\} + \cdots \end{aligned} \tag{156}$$

where

$$\begin{aligned} \xi_1^{(1)}(2\pi) &= -\int_0^{2\pi}[-3c(\varphi^*(\tau))^2\cos\tau + \zeta\sin\tau]\sin\tau\, d\tau = -\frac{\partial P}{\partial M_0} \\ \dot{\xi}_1^{(1)}(2\pi) &= \int_0^{2\pi}[-3c(\varphi^*(\tau))^2\cos\tau + \zeta\sin\tau]\cos\tau\, d\tau = \frac{\partial Q}{\partial M_0} \\ \xi_1^{(2)}(2\pi) &= -\int_0^{2\pi}[-3c(\varphi^*(\tau))^2\sin\tau - \zeta\cos\tau]\sin\tau\, d\tau = -\frac{\partial P}{\partial N_0} \\ \dot{\xi}_1^{(2)}(2\pi) &= \int_0^{2\pi}[-3c(\varphi^*(\tau))^2\sin\tau - \zeta\cos\tau]\cos\tau\, d\tau = \frac{\partial Q}{\partial N_0} \end{aligned} \tag{157}$$

From the first equation of Eq. (156) we see that an inversely unstable periodic solution cannot exist in Eq. (139). Substituting Eq. (157) into Eq. (156) we obtain the relations

$$\begin{aligned} \chi(1) &= \epsilon^2 \det \mathbf{A} + \epsilon^3\{\cdots\} + \cdots \\ a_2 &= 1 + \epsilon\ \mathit{trace}\ \mathbf{A} + \epsilon^3\{\cdots\} + \cdots \end{aligned} \tag{158}$$

where

$$\mathbf{A} = \begin{bmatrix} -\dfrac{\partial P}{\partial M_0} & \dfrac{\partial P}{\partial N_0} \\ -\dfrac{\partial Q}{\partial M_0} & \dfrac{\partial Q}{\partial N_0} \end{bmatrix} \tag{159}$$

Finally from Eqs. (143) and (146), we have

$$\begin{aligned} &\mathit{trace}\ \mathbf{A} = -2\zeta < 0 \\ &\det \mathbf{A} = a^2 + \zeta^2 - 3acr^2 + \frac{27}{16}c^2r^4 = \frac{db^2}{dr^2} \end{aligned} \tag{160}$$

Note that from the first equation of Eq. (160), we see that no completely unstable type of periodic solution exists in Eq. (139). Hence the stability of the periodic solution is determined as follows:

(a) If det $\mathbf{A} > 0$, that is, $db^2/dr^2 > 0$, then the periodic solution is a completely stable type: $_0D$.
(b) If det $\mathbf{A} < 0$, that is, $db^2/dr^2 < 0$, then the periodic solution is a directly unstable type: $_1D$.

Now we return to the characteristic curves shown in Fig. 22. Considering the above conditions we find the completely stable portion and the directly unstable portion on each curve ζ = const. The vertical tangency of the curves results at the stability limit, which is indicated by the thick curve. Starting from the small b of Fig. 22, the amplitude r increases slowly with increase of b. When the curve comes to the point with vertical tangency, a slight increase b will cause a discontinuous jump of r to the upper portion of the curve. With decreasing b, the amplitude r jumps down from the upper portion to the lower portion at another point with vertical tangency. Thus the process exhibits a hysteresis phenomenon (see Fig. 24). We refer to the periodic solution with larger amplitude as the resonant state and to the other with smaller amplitude as the nonresonant state. Similar hysteresis phenomenon is observed for the frequency characteristic curves illustrated in Fig. 23.

Averaging Method. Averaging method is another conventional method for studying periodic solution of quasilinear systems. Consider again Eq. (139) in normal form as

$$\begin{aligned} \dot{x} &= y \\ \dot{y} &= -x + \epsilon(b\cos t + ax - \zeta y - cx^3) = -x + \epsilon G(x, y, \epsilon, t) \end{aligned} \tag{161}$$

We assume an approximate periodic solution of Eq. (161) as

$$\begin{aligned} x(t) &= u(t)\cos t + v(t)\sin t \\ y(t) &= -u(t)\sin t + v(t)\cos t \end{aligned} \tag{162}$$

where $u(t)$ and $v(t)$ will be found slowly varying functions. Substituting Eq. (162) into Eq. (161), we have

$$\begin{aligned} \dot{u}(t) &= -\epsilon G(u\cos t + v\sin t,\ -u\sin t + v\cos t, \epsilon, t)\sin t \\ \dot{v}(t) &= \epsilon G(u\cos t + v\sin t,\ -u\sin t + v\cos t, \epsilon, t)\cos t \end{aligned} \tag{163}$$

Averaging the right-hand side of Eq. (163), we obtain

$$\begin{aligned} \dot{u}(t) &= -\frac{\epsilon}{2\pi}\int_0^{2\pi} \\ &\quad G(u\cos\tau + v\sin\tau, -u\sin\tau + v\cos\tau, \epsilon, \tau)\sin\tau d\tau \\ \dot{v}(t) &= -\frac{\epsilon}{2\pi}\int_0^{2\pi} \\ &\quad G(u\cos\tau + v\sin\tau, -u\sin\tau + v\cos\tau, \epsilon, \tau)\cos\tau d\tau \end{aligned} \tag{164}$$

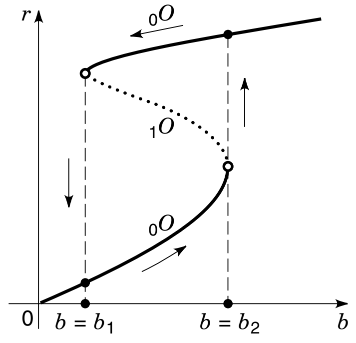

Figure 24. Jump and hysteresis phenomenon on an amplitude characteristic curve.

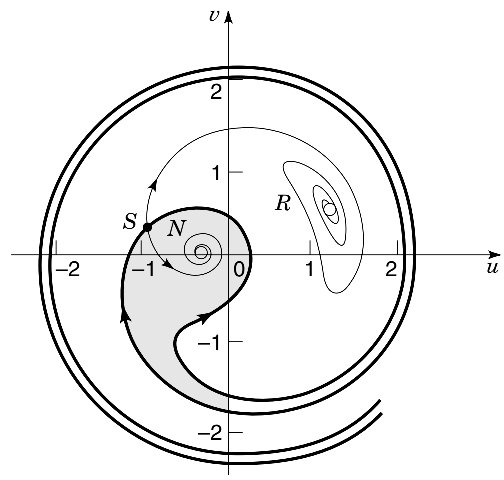

Figure 25. Phase portrait of Eq. (165) with $a = c = 1$, $\zeta = 0.1$, and $b = 0.3$.

That is, we have an autonomous equation

$$\begin{aligned} \dot{u} &= -\frac{\epsilon}{2}\left\{\zeta u + \left(a - \frac{3}{4}cr^2\right)v\right\} = -\frac{\epsilon}{2}P(u,v) \\ \dot{v} &= \frac{\epsilon}{2}\left\{\left(a - \frac{3}{4}cr^2\right)u - \zeta v + b\right\} = \frac{\epsilon}{2}Q(u,v) \end{aligned} \tag{165}$$

where $P(u, v)$ and $Q(u, v)$ are given in Eq. (143). An equilibrium point of Eq. (165) gives a periodic solution Eq. (162). Hence we have the correspondence between the equilibria of Eq. (165) and the periodic solutions of Eq. (161). Moreover, the phase portrait of Eq. (165) gives information about global behavior of the solutions of Eq. (161). Figure 25 shows a phase portrait of the case where three equilibria exist in Eq. (165). We see two sinks R and N corresponding to the resonant and nonresonant solutions, respectively. We also illustrate a saddle S whose stable manifold forms the basin boundary of two attractors.

References in This Section

The Poincaré map stated in this section is discussed in any books on nonlinear dynamics; for example, see Refs. 4, 9, and 12. Hyperbolicity of fixed point of the Poincaré map is introduced in Refs. 7 and 12. The classification of the hyperbolic fixed point is found in Refs. 17–21. Various numerical methods are well treated in Refs. 22 and 23. Various nonlinear resonances—that is, subharmonic resonance and higher harmonic resonance as well as harmonic resonance—are treated in the standard books on nonlinear oscillations (see Refs. 3–6). For the perturbation method stated in the last paragraph, see Ref. 24. Practical applications of the averaging method are found in Ref. 3.

BIFURCATIONS OF EQUILIBRIA AND PERIODIC STATES

When the system parameter λ varies, the qualitative properties of the state space may change at $\lambda = \lambda_0$. We may observe the generation or extinction of a couple of equilibria or fixed points, the branching of new equilibria or fixed or periodic points, and the change of a topological type of equilibrium point or fixed point. We call these phenomena the bifurcation of equilibrium point or fixed point and call $\lambda = \lambda_0$ a bifurcation value. These bifurcations occur when the hyperbolicity is violated at $\lambda = \lambda_0$, which corresponds to the critical distribution of the eigenvalues or multipliers of the characteristic equation. Typical bifurcation is observed under the single bifurcational condition and is called generic or codimension one bifurcation. Mathematically, we have to discuss the normal form theory of vector fields, the center manifold theorem, and the unfolding theory. For our circuit application, however, the bifurcation condition is the most important to study bifurcations of concrete circuit examples. Thus we will introduce only some basic results of bifurcation problems of equilibrium point or fixed point. We will discuss the bifurcation of periodic state as the bifurcation of fixed points of the Poincaré map.

Bifurcation of Equilibrium Point

Consider an autonomous system

$$\dot{\mathbf{x}} = \mathbf{f}(\mathbf{x}, \lambda), \qquad \mathbf{x} \in \mathbf{R}^n,\ \lambda \in \mathbf{R}^m \tag{166}$$

where $\mathbf{x} \in \mathbf{R}^n$ is a state vector and $\lambda \in \mathbf{R}^m$ is a system parameter. Suppose that $\mathbf{x}_0 \in \mathbf{R}^n$ is an equilibrium point of Eq. (166):

$$\mathbf{f}(\mathbf{x}_0, \lambda) = \mathbf{0} \tag{167}$$

The Jacobian matrix of Eq. (167) is given by

$$D\mathbf{f}(\mathbf{x}_0, \lambda) = \mathbf{A}(\lambda) \tag{168}$$

The characteristic equation is written as

$$\begin{aligned} \chi(\mu) &= \det(\mu \mathbf{I}_n - \mathbf{A}(\lambda)) \\ &= \mu^n + a_1\mu^{n-1} + \cdots + a_{n-1}\mu + a_n = 0 \end{aligned} \tag{169}$$

Hyperbolicity is violated at a bifurcation value $\lambda = \lambda_0$ when the Jacobian $\mathbf{A} = D\mathbf{f}(\mathbf{x}_0, \lambda)$ becomes singular or a couple of characteristic roots become purely imaginary numbers. In the former case we observe the number of equilibria may change, whereas in the latter case the type of equilibrium point may change; that is, the stability may change and new periodic orbit will be generated. We assume that along the variation of λ, the above location of characteristic root actually changes, that is,

$$\left.\frac{d\,\mathrm{Re}(\mu)}{d\lambda}\right|_{\lambda=\lambda_0} \neq 0 \tag{170}$$

Then the generic bifurcation of equilibrium point is the two cases described below.

Tangent Bifurcation of Equilibrium Point. If one of the characteristic roots becomes zero at the bifurcation parameter $\lambda = \lambda_0$, then the generation or extinction of a couple of equilibria occurs. Symbolically we have the following bifurcation relation:

$${}_kO + {}_{k+1}O \Leftrightarrow \varnothing \qquad (k = 0, 1, \ldots, n-1) \tag{171}$$

where the symbol $\Leftrightarrow$ indicates the relation before and after the bifurcation and $\emptyset$ denotes the extinction of equilibria. The plus sign appearing in the left-hand side of the relation means that before the bifurcation we have a couple of equilibria of the type ${}_kO$ and ${}_{k+1}O$. At the bifurcation value $\lambda = \lambda_0$ these two equilibria coalesce into one nonhyperbolic equilibrium point, and after the bifurcation they disappear completely. The bifurcation condition is then given by

$$\chi(0) = \det(0 - \mathbf{A}(\lambda)) = a_n = 0 \tag{172}$$

Geometrically in the parameter space $\mathbf{R}^m$, Eq. (172) gives a hypersurface with the dimension $m - 1$. Hence this bifurcation is called a codimension one bifurcation. The tangent bifurcation is also called a saddle-node bifurcation, a fold bifurcation, or a turning point in various contexts.

The Hopf Bifurcation. This bifurcation is observed if a couple of characteristic roots becomes purely imaginary numbers at $\lambda = \lambda_0$. The stability of the equilibrium point changes and a limit cycle appear or disappear after the bifurcation. Symbolically we have the following relation:

$$\begin{aligned} &{}_kO \Leftrightarrow {}_{k+2}O + LC({}_kD) \qquad (k = 0, 1, \ldots, n-2) \\ &{}_kO + LC({}_{k+1}D) \Leftrightarrow {}_{k+2}O \qquad (k = 0, 1, \ldots, n-2) \end{aligned} \tag{173}$$

where $LC({}_kD)$ denotes a limit cycle whose type of the corresponding fixed point of the Poincaré map is ${}_kD$. The first relation shows that before the bifurcation a k-dimensionally unstable hyperbolic equilibrium point exists, and after the bifurcation the equilibrium point becomes a $(k + 2)$-dimensionally unstable and k-dimensionally unstable limit cycle of the type ${}_kD$ appears. If $k = 0$, then a sink becomes two-dimensionally unstable and an orbitally stable limit cycle appears. This type of Hopf bifurcation is called a *supercritical type,* whereas the second relation shows a *subcritical type* (see Fig. 26). The bifurcation condition is then given by

$$\chi(j\omega) = \det(j\omega\mathbf{I}_n - \mathbf{A}(\lambda)) = 0 \tag{174}$$

where $j = \sqrt{-1}$. This condition gives two relations derived from the real and imaginary parts. By eliminating the unknown ω, which gives the angular frequency of the bifurcated limit cycle, we obtain a single condition. Hence this is also a codimension one bifurcation.

Example 8. 1. *The Hopf bifurcation for low-dimensional systems.* For low-dimensional systems, the condition Eq. (174) is easily obtained as follows.

(a) *Two-dimensional system.* The condition is given by

$$\chi(j\omega) = (j\omega)^2 + j\omega a_1 + a_2 = 0 \tag{175}$$

Hence we have

$$a_1 = 0, \quad a_2 = \omega^2 > 0; \qquad \omega = \sqrt{a_2} \tag{176}$$

(b) *Three-dimensional system.* The condition is given by

$$\chi(j\omega) = (j\omega)^3 + a_1(j\omega)^2 + j\omega a_2 + a_3 = 0 \tag{177}$$

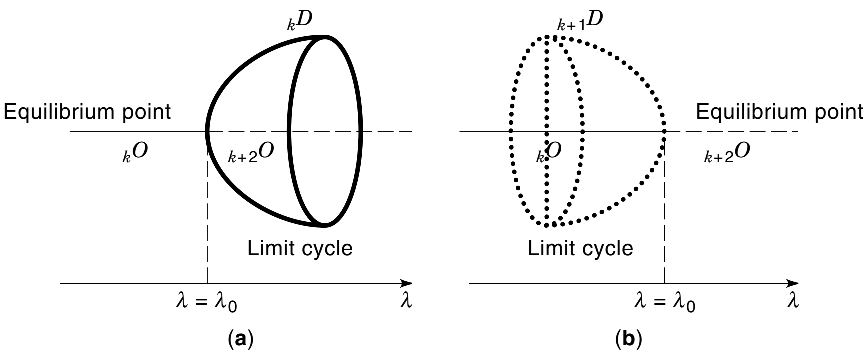

Figure 26. Schematic diagram of Hopf bifurcation. (a) Supercritical case, (b) subcritical case.

Hence we have

$$-a_1a_2 + a_3 = 0, \quad a_2 > 0; \qquad \omega = \sqrt{a_2} \tag{178}$$

(c) *Four-dimensional system.* The condition is given by

$$\chi(j\omega) = (j\omega)^4 + a_1(j\omega)^3 + a_2(j\omega)^2 + j\omega a_3 + a_4 = 0 \tag{179}$$

Hence we have

$$a_4^2 + a_1^2(a_4 - a_2) = 0, \quad \frac{a_4}{a_2} > 0; \qquad \omega = \sqrt{\frac{a_4}{a_2}} \tag{180}$$

2. *Bifurcation diagram of equilibria of Eq. (165).* Consider the equilibria of Eq. (165). The equilibrium point satisfies Eq. (146). Figure 27 shows the surface defined by Eq. (146) in the (ζ, b, r) space, where we set $a = c = 1$. Projecting this surface into the (b, r) plane, we have the amplitude characteristic curve as illustrated in Fig. 22. On the other hand, by projecting the surface into the parameter (b, ζ) plane, we obtain a diagram, called a *bifurcation diagram,* which indicates the tangent bifurcation curve (see also Fig. 28). The diagram shows the region in which three or one equilibrium points exist, and on the boundary curves t_1, t_2 we have the tangent bifurcation. Note that at the cusp point C in Fig. 28 we have a degenerate equilibrium point, that is, a codimension two bifurcation point.

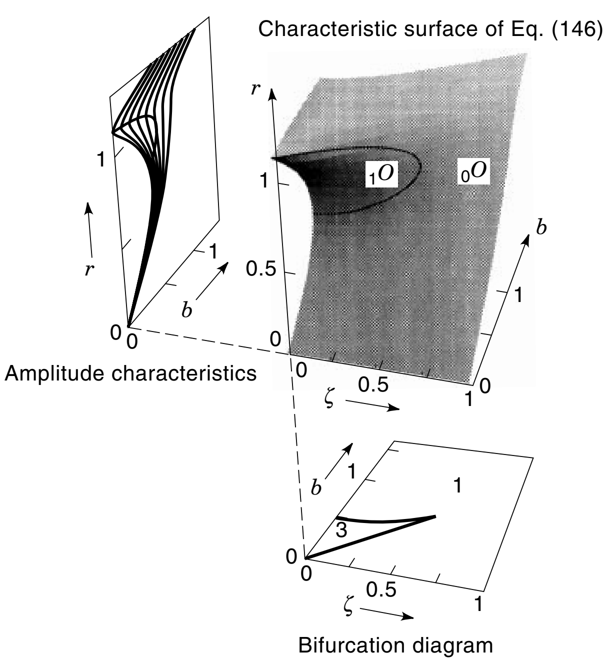

Figure 27. Characteristic surface of Eq. (146) with amplitude characteristic curves and bifurcation diagram.

Bifurcation of a Fixed Point

Consider the Poincaré map T defined by Eq. (109). T depends on the parameter $\lambda \in \mathbf{R}^m$ so that a bifurcation of a fixed point may occur under the change of λ. Suppose that $\mathbf{x}_0 \in \mathbf{R}^n$ is a fixed point of T:

$$\mathbf{x}_0 - T(\mathbf{x}_0) = \mathbf{0} \tag{181}$$

The characteristic equation is written as

$$\begin{aligned}\chi(\mu) &= \det(\mu \mathbf{I}_n - DT(\mathbf{x}_0)) \\ &= \mu^n + a_1\mu^{n-1} + \cdots + a_{n-1}\mu + a_n = 0\end{aligned} \tag{182}$$

Hyperbolicity is violated at a bifurcation value $\lambda = \lambda_0$ when the characteristic multiplier has the critical distribution: $\mu = +1$, $\mu = -1$, or $\mu = e^{j\theta}$. Hence we have actually three different types of codimension one bifurcations for fixed point of T.

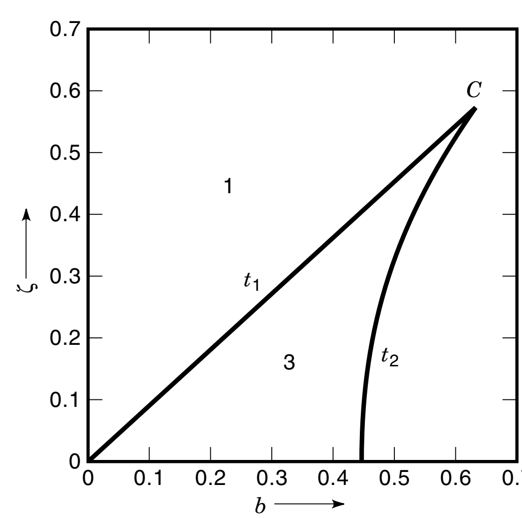

Figure 28. Bifurcation diagram of equilibria. Tangent bifurcation occurs on the curves t_1 and t_2, and the cusp point C is a degenerate tangent bifurcation point.

Tangent Bifurcation of Fixed Point. Under the change of parameter λ, at $\lambda = \lambda_0$ the generation or extinction of a couple of fixed points occurs. The types of bifurcation are

$$\begin{aligned} \varnothing &\Leftrightarrow {}_{k-1}D + {}_kD \\ \varnothing &\Leftrightarrow {}_{k-1}I + {}_kI \end{aligned} \tag{183}$$

where $\varnothing$ denotes the extinction of fixed points and the symbol $\Leftrightarrow$ indicates the relation before and after the bifurcation. This type of bifurcation is observed if one of the multipliers of Eq. (182) satisfies the condition $\mu = 1$ or, equivalently,

$$\begin{aligned} \chi(\mu) &= \det(\mathbf{I}_n - DT(\mathbf{x}_0)) \\ &= 1 + a_1 + \cdots + a_{n-1} + a_n = 0 \end{aligned} \tag{184}$$

and the remainder of the characteristic multipliers lies off the unit circle in the complex plane.

Period-Doubling Bifurcation. If a real characteristic multiplier passes through the point $(-1, 0)$ in the complex plane, then the original fixed point changes its type and 2-periodic points are branching. This bifurcation is called a *period-doubling bifurcation.* The types of bifurcation are

$$\begin{aligned} {}_kD &\Leftrightarrow {}_{k+1}I + 2\,{}_kD^2 \\ {}_kD &\Leftrightarrow {}_{k-1}I + 2\,{}_kD^2 \\ {}_kI &\Leftrightarrow {}_{k+1}D + 2\,{}_kD^2 \\ {}_kI &\Leftrightarrow {}_{k-1}D + 2\,{}_kD^2 \end{aligned} \tag{185}$$

where $2\,{}_kD^2$ indicates two numbers of 2-periodic point of the type D. This type of bifurcation is observed if $\mu = -1$ or, equivalently,

$$\begin{aligned} \chi(-1) &= \det(\mu\mathbf{I}_n - DT(\mathbf{x}_0)) \\ &= (-1)^n + a_1(-1)^{n-1} + \cdots - a_{n-1} + a_n = 0 \end{aligned} \tag{186}$$

The Neimark–Sacker Bifurcation. Similar to the Hopf bifurcation for equilibrium point, a fixed point becomes unstable and there may appear an invariant closed curve of the Poincaré map. Here the invariant closed curve C is a closed curve in $\mathbf{R}^n$ such that $T(C) = C$, which corresponds to doubly periodic oscillation in the original periodic nonautonomous system. This bifurcation indeed occurs if a pair of the characteristic multipliers μ and $\overline{\mu}$ pass transversally through the unit circle except for the points (1, 0) and $(-1, 0)$. The types of the bifurcation are

$$\begin{aligned} {}_kD &\Leftrightarrow {}_{k+2}D + ICC \\ {}_kD &\Leftrightarrow {}_{k-2}D + ICC \\ {}_kI &\Leftrightarrow {}_{k+2}D + ICC \\ {}_kI &\Leftrightarrow {}_{k-2}D + ICC \end{aligned} \tag{187}$$

where ICC indicates an invariant closed curve of the Poincaré map T. The condition for this type of bifurcation is given by

$$\begin{aligned} \chi(e^{j\theta}) &= \det(e^{j\theta}\mathbf{I}_n - DT(\mathbf{x}_0)) \\ &= e^{jn\theta} + a_1 e^{j(n-1)\theta} + \cdots + a_{n-1}e^{j\theta} + a_n = 0 \end{aligned} \tag{188}$$

Hence by eliminating θ in Eq. (188) we have the single condition

$$\chi_{NS}(\mathbf{x}_0, \lambda) = 0 \tag{189}$$

Note that in this case we need an additional inequality satisfying the condition: $|\cos\,\theta| < 1$.

Example 9. The Neimark–Sacker bifurcation for two- or three-dimensional systems. First consider nonautonomous systems.

1. *Two-dimensional system.* The condition is given by

$$\chi(e^{j\theta}) = e^{j2\theta} + a_1 e^{j\theta} + a_2 = 0 \tag{190}$$

That is,

$$\begin{aligned} \cos 2\theta + a_1\cos\theta + a_2 &= 0, \\ \sin 2\theta + a_1 \sin\theta &= 0 \end{aligned} \tag{191}$$

Hence we have

$$a_2 = 1, \qquad -2 < a_1 < 2 \tag{192}$$

2. *Three-dimensional system.* The condition is given by

$$\chi(e^{j\theta}) = e^{j3\theta} + a_1 e^{j2\theta} + a_2 e^{j\theta} + a_3 = 0 \tag{193}$$

or equivalently

$$a_1(a_3 - a_1) + a_2 = 1, \qquad -2 < a_3 - a_1 < 2 \tag{194}$$

Second consider autonomous systems. In this case the characteristic equation has at least one unity multiplier. Thus we factor the characteristic equation as

$$\chi(\mu) = \mu^n + a_1\mu^{n-1} + \cdots + a_{n-1}\mu + a_n = (\mu - 1)\chi_A(\mu) = 0 \tag{195}$$

where

$$\chi_A(\mu) = \mu^{n-1} + b_1\mu^{n-2} + \cdots + b_{n-1}, \qquad b_k = 1 + \sum_{i=1}^{k} a_i \tag{196}$$

The bifurcation condition is then given by using a new characteristic equation:

$$\chi_A(\mu) = \mu^{n-1} + b_1\mu^{n-2} + \cdots + b_{n-1} = 0 \tag{197}$$

For the three-dimensional system the condition is given by

$$\begin{aligned} \chi_A(e^{j\theta}) &= e^{j2\theta} + b_1 e^{j\theta} + b_2 \\ &= e^{j2\theta} + (a_1 + 1)e^{j\theta} + (a_2 + a_1 + 1) = 0 \end{aligned} \tag{198}$$

or, equivalently,

$$a_2 + a_1 = 0, \qquad -3 < a_1 < 1 \tag{199}$$

Numerical Method of Computation

The numerical determination of the codimension one bifurcation value $\lambda = \lambda_0$ and the location of the nonhyperbolic fixed point is accomplished by solving the fixed point equation and the bifurcation condition, simultaneously. The unknown variables are the location of the fixed point and one of the components of λ. The computation is achieved by Newton's method, and the Jacobian matrix is evaluated by the solutions of the variational equations with respect to the initial conditions as well as the system parameters (see Theorem 2 and Remark 3).

Harmonic Synchronization of Forced Rayleigh Equation

Let us consider the harmonic synchronization or entrainment of Rayleigh's equation with a sinusoidal external force:

$$\begin{aligned}\dot{x} &= y\\ \dot{y} &= -x + \epsilon(1-\gamma y^2)y + \epsilon B\cos\nu t\end{aligned} \tag{200}$$

Assume that the periodic solution of Eq. (200) as

$$\begin{aligned}x(t) &= u(t)\cos\nu t + v(t)\sin\nu t\\ y(t) &= -u(t)\sin\nu t + v(t)\cos\nu t\end{aligned} \tag{201}$$

By using the averaging method we have an autonomous equation:

$$\begin{aligned}\dot{u} &= \frac{\epsilon}{2}\left[\left(1-\frac{3}{4}\gamma r^2\right)u - \sigma v\right] = f(u,v)\\ \dot{v} &= \frac{\epsilon}{2}\left[\sigma u + \left(1-\frac{3}{4}\gamma r^2\right)v + B\right] = g(u,v)\end{aligned} \tag{202}$$

where

$$r^2 = u^2 + v^2, \qquad \sigma = \frac{2(\nu-1)}{\epsilon} \tag{203}$$

Hence the equilibrium point is given by

$$\begin{aligned}\left(1-\frac{3}{4}\gamma r^2\right)u - \sigma v &= 0\\ \sigma u + \left(1-\frac{3}{4}\gamma r^2\right)v &= -B\end{aligned} \tag{204}$$

That is, the amplitude satisfies the relation

$$\left[\left(1-\frac{3}{4}\gamma r^2\right)^2 + \sigma^2\right]r^2 = B^2 \tag{205}$$

At the equilibrium point the Jacobian matrix becomes

$$\begin{bmatrix}\dfrac{\partial f}{\partial u} & \dfrac{\partial f}{\partial v}\\ \dfrac{\partial g}{\partial u} & \dfrac{\partial g}{\partial v}\end{bmatrix} = \frac{\epsilon}{2}\begin{bmatrix}1-\dfrac{3}{4}\gamma(3u^2+v^2) & -\dfrac{3}{2}\gamma uv - \sigma\\ -\dfrac{3}{2}\gamma uv + \sigma & 1-\dfrac{3}{4}\gamma(u^2+3v^2)\end{bmatrix} \tag{206}$$

Thus the characteristic equation is given by

$$\chi(\mu) = \begin{vmatrix}\dfrac{\partial f}{\partial u} - \mu & \dfrac{\partial f}{\partial v}\\ \dfrac{\partial g}{\partial u} & \dfrac{\partial g}{\partial v} - \mu\end{vmatrix} = \mu^2 + a_1\mu + a_2 = 0 \tag{207}$$

where

$$\begin{aligned}a_1 &= 3\gamma r^2 - 2\\ a_2 &= \sigma^2 + 1 - 3\gamma r^2 + \frac{27}{16}\gamma^2 r^4 = \sigma^2 + \left(1-\frac{3}{4}\gamma r^2\right)\left(1-\frac{9}{4}\gamma r^2\right)\end{aligned} \tag{208}$$

Hence we can determine the type of equilibrium point by the sign of the coefficients in Eq. (208) as in Example 5(1). Figure 29 shows the characteristic surface of Eq. (205) in the (σ, B, r) space. Topological type of the equilibrium point is indicated on the surface. Projecting the surface into the (σ, B) plane we have the bifurcation diagram for the equilibria. The projected plane is also shown in Fig. 30(a), where the type of equilibrium point is indicated in each region. Roughly speaking, harmonic synchronization occurs in the region in which a stable ${}_0O$ equilibrium point exists. The curves t_1, t_2,, and t_3 indicate the tangent bifurcation curves joined at cusp points c_1 and c_2. The curves h_1 and h_2 illustrate the Hopf bifurcation, which join the tangent bifurcation curves at points P and Q [see Fig. 30(b)]. If we decrease B transversally across the curves h_1 and h_2, we see a supercritical Hopf bifurcation. Hence below the curves h_1 and h_2 we have a stable limit cycle. This state corresponds to an asynchronous state—that is, a beat oscillation or quasiperiodic oscillation.

Parametric Excitation. 1. *Mathieu's equation.* Consider the second-order linear system, called *Mathieu's equation,*

$$\ddot{x} + (a + b\cos 2t)x = 0 \tag{209}$$

or, equivalently,

$$\dot{\mathbf{x}} = \mathbf{A}(t)\mathbf{x} \tag{210}$$

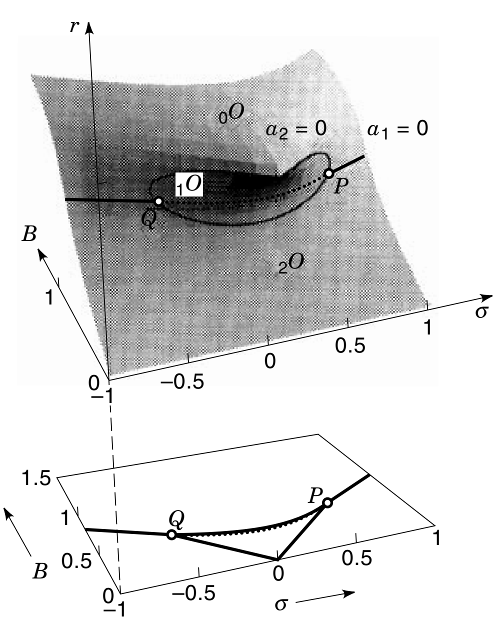

Figure 29. Characteristic surface of Eq. (205) and projected bifurcation diagram.

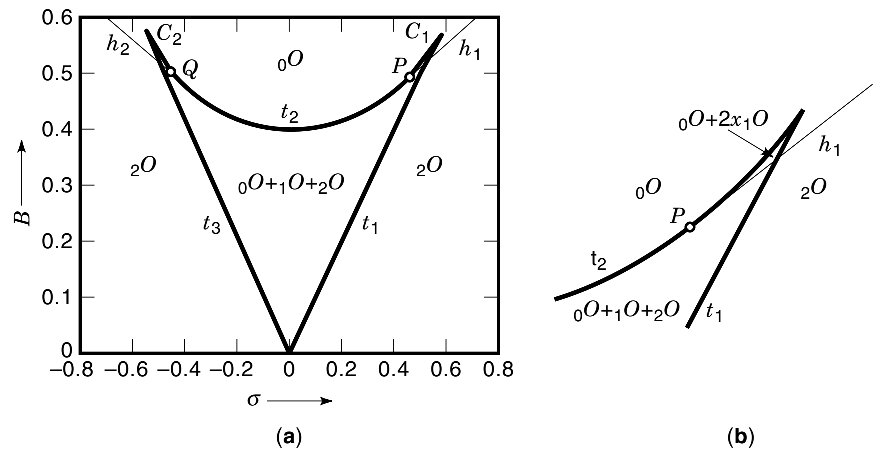

Figure 30. (a) Bifurcation diagram of equilibria of Eq. (202) and (b) its partially enlarged diagram.

where

$$\mathbf{x} = \begin{bmatrix} x \\ y \end{bmatrix}, \qquad \mathbf{A}(t) = \begin{bmatrix} 0 & 1 \\ -(a + b\cos 2t) & 0 \end{bmatrix} \tag{211}$$

The origin is a stationary solution. Hence we will discuss its stability. Let the principal fundamental matrix solution be

$$\Phi(t) = \begin{bmatrix} \varphi_1(t) & \varphi_2(t) \\ \psi_1(t) & \psi_2(t) \end{bmatrix} \tag{212}$$

As the period of the coefficient is π, the Poincaré map T is defined by

$$T = \Phi(\pi): \qquad \mathbf{R}^2 \to \mathbf{R}^2; \quad \mathbf{x}_0 \mapsto \mathbf{x}_1 = \Phi(\pi)\mathbf{x}_0 \tag{213}$$

The characteristic equation is then given by

$$\chi(\mu) = \det[\mu \mathbf{I}_2 - \Phi(\pi)] = \mu^2 - m\mu + 1 = 0 \tag{214}$$

where we put

$$m = \varphi_1(\pi) + \psi_2(\pi) = \mu_1 + \mu_2 \tag{215}$$

and use the relation

$$\chi(0) = \mu_1\mu_2 = \det\Phi(\pi) = \det\Phi(0)e^{\int_0^\pi \mathrm{trace}\mathbf{A}(\tau)\,d\tau} = 1 \tag{216}$$

Hence we have the following results:

(a) If $m > 2$, then $0 < \mu_1 < 1 < \mu_2$ and the origin is a directly unstable: $_0D$. From the Floquet theorem we have the general solution of the form

$$x(t) = c_1 e^{\nu_1 t}\phi(t) + c_2 e^{\nu_2 t}\psi(t) \tag{217}$$

where c_1 and c_2 are arbitrary constants, $\nu_1 = (1/\pi)\log \mu_1$, $\nu_2 = (1/\pi)\log \mu_2$, and $\phi(t)$ and $\psi(t)$ are periodic functions with period π.

(b) If $m < -2$, then $\mu_1 < -1 < \mu_2 < 0$ and the origin is an inversely unstable: $_1I$. The general solution has the same form as Eq. (217), but $\nu_1 = (1/2\pi)\log \mu_1^2$, $\nu_2 = (1/2\pi)\log \mu_2^2$, and $\phi(t)$ and $\psi(t)$ are periodic functions with period 2π.

(c) If $|m| < 2$, then the origin is a nonhyperbolic fixed point—that is, a center-type fixed point. The general solution is then a doubly periodic function. In the last case the characteristic multipliers lie on the unit circle in the complex plane:

$$\mu_1 = \overline{\mu_2} = \exp(j\theta), \qquad j = \sqrt{-1}, \qquad \theta = tan^{-1}\left\{\frac{\sqrt{4-m^2}}{m}\right\} \tag{218}$$

Note that Eq. (210) is a lossless system so that the Poincaré map of Eq. (213) is the area-preserving map on $\mathbf{R}^2$. The stability chart is a diagram of the (a, b) parameter plane, which shows contour curves of m and where we find the origin being a directly hyperbolic, an inversely hyperbolic, or a nonhyperbolic type. By numerical integration we can easily obtain the value of Eq. (215). Figure 31 shows the contour curves for different values of m. The shaded regions indicate the regions where the origin becomes the $_1D$ or $_1I$ type of instability. These regions approach the a axis near the point $a = k^2$, $k = 1, 2, \ldots$.

2. *Damped Mathieu's equation with a cubic nonlinear restoring force.* Consider the damped nonlinear system

$$\ddot{x} + k\dot{x} + (a + b\cos 2t)x + x^3 = 0 \tag{219}$$

or, equivalently,

$$\begin{aligned} \dot{x} &= y \\ \dot{y} &= -k\dot{x} - (a + b\cos 2t)x - x^3 \end{aligned} \tag{220}$$

The variational equation for the origin becomes

$$\ddot{\xi} + k\dot{\xi} + (a + b\cos 2t)\xi = 0 \tag{221}$$

The characteristic equations has the form

$$\chi(\mu) = \det[\mu \mathbf{I}_2 - \Phi(\pi)] = \mu^2 - m\mu + a_2 = 0 \tag{222}$$

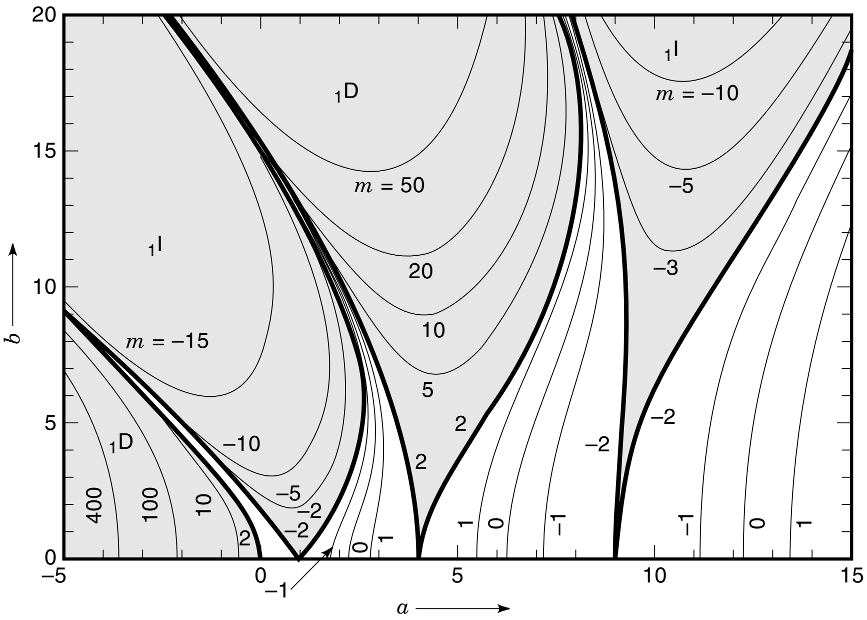

Figure 31. Stability chart or contour m chart of Eq. (209). The origin becomes unstable of the type $_1D$ or $_1I$ in the shaded region.

where

$$a_2 = \chi(0) = \det\Phi(\pi) = \det\Phi(0)e^{-k\pi} < 1 \tag{223}$$

Hence the origin is a completely stable, a directly unstable, or an inversely unstable fixed point of the time π Poincaré map. Parametric excitation occurs in the parameter regions in which the origin becomes an inversely unstable or a directly unstable fixed point. Figure 32 shows the bifurcation diagram near the first unstable region just above $a = 1$. The white region and the shaded region indicate that the origin becomes a completely stable and an inversely unstable fixed point, respectively. On the curves P_1 and P_2 we have a period-doubling bifurcation of the origin. That is, two 2-periodic points branch off from the origin. Changing parameters from the area A to B, we see that two completely stable 2-periodic points branch off; see the phase portrait of the Poincaré map of Fig. 33(a). This is the typical parametric excitation phenomenon, also called the parametric resonance. Stable 2-periodic points $_0D_1^2$ and $_0D_2^2 = T(_0D_1^2)$ have the period 2π which is the double period of the injected pumping signal. Traversing the curve P_2 from the region B to C, we observe that two directly unstable 2-periodic points branch off from the origin and the origin itself becomes a completely stable fixed point. Hence in the region C we have the phase portrait shown in Fig. 33(b). On the tangent bifurcation curve T, 2-periodic points $_0D_1^2$ and $_1D_1^2$, (and also $_0D_2^2$ and $_1D_2^2$) coalesce and disappear in the region A below the curve T.

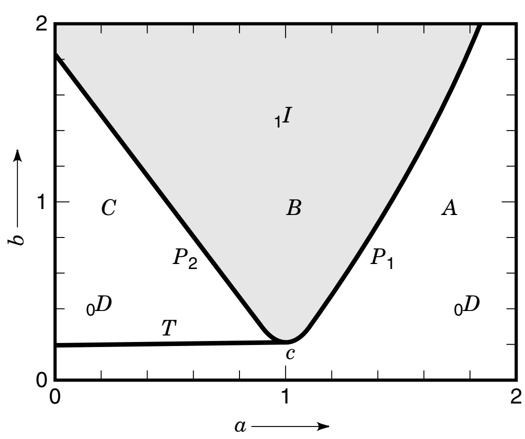

Figure 32. Bifurcation diagram of Eq. (219) with $k = 0.1$. Curves P_1 and P_2 indicate the period-doubling bifurcation of the origin, and T denotes the tangent bifurcation of 2-periodic points.

References in This Section

Many books are available on bifurcation theory. We refer to only a few of them: Refs. 7–9, 25, and 26. For the higher-order bifurcations—that is, codimension two bifurcations—see Refs. 9, 26, and 27. Various numerical methods are stated in Refs. 21 and 26–28. Harmonic synchronization is analyzed in Refs. 3, 6, and 9. Mathieu's equation and more generally the linear periodic differential equations are well surveyed in

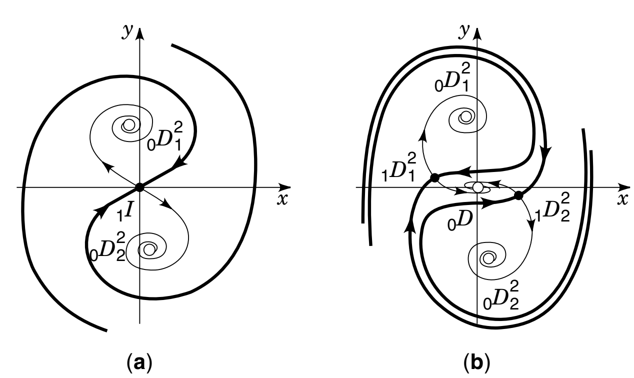

Figure 33. Phase portrait of the time π Poincaré map of Eq. (219). (a) $k = 0.1$, $a = b = 1.0$; (b) $k = 0.1$, $a = b = 0.54$.

Ref. 29. Parametric excitation is found in Refs. 5, 8, 30, and 31.

HOMOCLINIC STRUCTURE OF NONLINEAR CIRCUIT DYNAMICS

Thus far in the previous sections we have discussed local properties of circuit dynamics. Global properties, such as the geometrical behavior of invariant manifolds of a saddle-type equilibrium point or a fixed point, the abrupt disappearance of attractors, and the appearance of chaotic states, really reflect nonlinearity of dynamical systems. These properties relate a wide range movement of state in state-space and long-term behavior of a trajectory. In this section we extract two topics on the global structure of phase portraits. First we illustrate the separatrix loop in two-dimensional autonomous systems. Second we discuss the homoclinic points and related chaotic states in Duffing's equation. These simple examples illustrate the complexity of the global behavior of nonlinear systems.

Separatrix Loop

Two-dimensional autonomous systems in the plane have been studied for many years and exhibit many interesting properties. To see the global structure of a phase portrait, it is important to know the behavior of stable and unstable orbits of saddle points. In fact in planar systems, the candidates of invariant steady states are known as equilibria, periodic orbits, or a set of saddles and trajectories connecting them if they exist. The latter are called saddle connections or heteroclinic orbits if they connect distinct saddles, and they are called separatrix loop or homoclinic orbit if they connect a saddle to itself (see Fig. 34). It is known that these connections are violated under small variation of parameters λ. That is, they are structually unstable and if such a connection exists at $\lambda = \lambda_0$, then a global bifurcation may occur by changing parameter λ. An example of such a bifurcation is the disappearance of a limit cycle associated with a separatrix loop, which is shown in Fig. 35. A limit cycle approaches the stable and unstable orbit of a saddle in Fig. 35(a), and at $\lambda = \lambda_0$ the cycle coalesces into and forms the separatrix loop in Fig. 35(b). Afterward the bifurcation the cycle disappears completely as in Fig. 35(c). Thus in the process of this bifurcation the phase portrait changes globally and the oscillatory state corresponding to the stable limit cycle abruptly disappears at $\lambda = \lambda_0$.

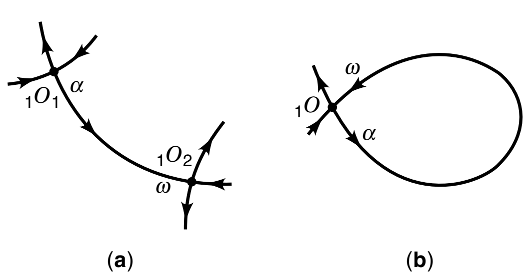

Figure 34. Schematic diagram of a saddle to saddle orbit. (a) A saddle connection orbit, or heteroclinic orbit; (b) a separatrix loop, or homoclinic orbit.

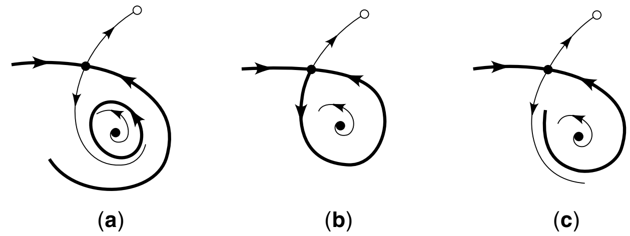

Figure 35. Bifurcation of a separatrix loop. A stable limit cycle shown in (a) disappears after this bifurcation shown in (c).

Example 10. *Duffing–Rayleigh equation.* Consider a forced oscillator described by

$$\begin{aligned} \dot{x} &= y \\ \dot{y} &= -x + \epsilon\{(1-\gamma y^2)y - cx^3 + B\cos\nu t\} \end{aligned} \tag{224}$$

Comparing with Eq. (200), Eq. (224) has a cubic nonlinear restoring term and is called the *Duffing–Rayleigh equation.* Assuming the harmonic oscillation as Eq. (201) and using the averaging method we have the autonomous system:

$$\begin{aligned} \dot{u} &= \frac{\epsilon}{2}\left[\left(1-\frac{3}{4}\gamma r^2\right)u - \left(\sigma - \frac{3}{4}cr^2\right)v\right] \\ \dot{v} &= \frac{\epsilon}{2}\left[\left(\sigma - \frac{3}{4}cr^2\right)u + \left(1-\frac{3}{4}\gamma r^2\right)v + B\right] \end{aligned} \tag{225}$$

where we put the amplitude and the detuning as

$$r^2 = u^2 + v^2, \qquad \sigma = \frac{2(\nu-1)}{\epsilon} \tag{226}$$

Then the equilibrium point satisfies the relation

$$\left[\left(1-\frac{3}{4}\gamma r^2\right)^2 + \left(\sigma - \frac{3}{4}cr^2\right)^2\right]r^2 = B^2 \tag{227}$$

Figure 36 shows the bifurcation diagram of the equilibria given by Eq. (227). The diagram is similar to that of Fig. 30. But tangent bifurcation curves are right side up so that we

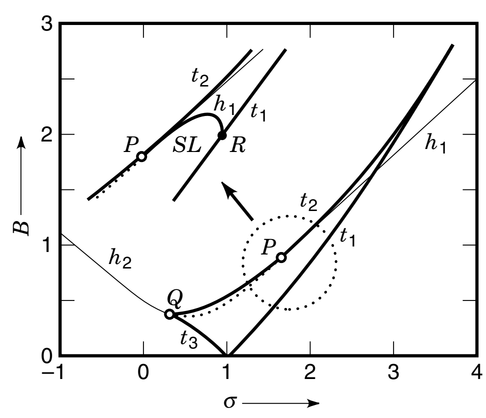

Figure 36. Bifurcation diagram of equilibria of Eq. (227). The curves t, h, and SL denote the tangent bifurcation, the Hopf bifurcation, and the bifurcation of separatrix loop, respectively.

can more clearly discuss the region near the intersection point P of the tangent bifurcation curve t_2 and the Hopf bifurcation curve h_1. Actually from the point P to the point R on the curve t_1 there exists a bifurcation curve SL on which we have a separatrix loop. Figure 37 is a schematic diagram of the phase portraits in each region. The point P is a degenerate bifurcation point (i.e., t_2 and h_1 meet at this point) and is called the Bogdanov–Takens bifurcation point. The appearance of separatrix loop on SL suggests that in the original system, Eq. (224), there exist homoclinic points of the time $2\pi/\nu$ Poincaré map. This phenomenon will be discussed in the next section.

Homoclinic Point

Now we consider the phase portrait of the Poincaré map. We focus our attention to the behavior of invariant manifolds stated in Remark 5(1) [see Eq. (124)] and its related property. For simplicity consider a two-dimensional periodic nonautonomous system defined by Eq. (107):

$$\dot{\mathbf{x}} = \mathbf{f}(t, \mathbf{x}, \lambda), \qquad \mathbf{x} \in \mathbf{R}^2, \lambda \in \mathbf{R}^m \tag{228}$$

where $\mathbf{x} = (x, y) \in \mathbf{R}^2$ is a state vector and $\lambda \in \mathbf{R}^m$ is a system parameter. We assume that $\mathbf{f}$ is periodic in t with period 2π: $\mathbf{f}(t, \mathbf{x}, \lambda) = \mathbf{f}(t + 2\pi, \mathbf{x}, \lambda)$ for all $t \in \mathbf{R}$. Let $\mathbf{x}(t)$ be a solution $\mathbf{x}(t) = \varphi(t, \mathbf{x}_0, \lambda)$ with $\mathbf{x}(0) = \varphi(0, \mathbf{x}_0, \lambda) = \mathbf{x}_0$. Recall that we define the time 2π mapping as the Poincaré map:

$$\begin{aligned} T: \qquad \mathbf{R}^2 \to \mathbf{R}^2; \quad \mathbf{x}_0 = (x_0, y_0) \mapsto \mathbf{x}_1 &= (x_1, y_1) \\ &= T(\mathbf{x}_0) = \varphi(2\pi, \mathbf{x}_0, \lambda) \end{aligned} \tag{229}$$

If a solution $\mathbf{x}(t) = \varphi(t, \mathbf{x}_0, \lambda)$ is periodic with period 2π, then the initial state $\mathbf{x}_0$ is a fixed point of the map T. Recall also that a saddle-type fixed point—that is, a directly unstable or an inversely unstable fixed point—has a stable manifold and an unstable manifold defined by Eq. (124). In two-dimensional case, these manifolds are curves in the phase portrait of T. For example, if the point P is a directly unstable type

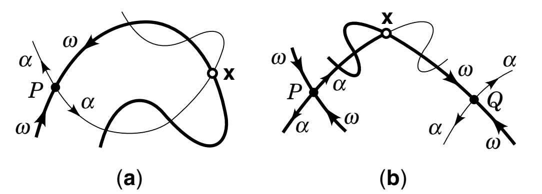

Figure 38. Invariant curves of saddle-type fixed points and doubly asymptotic points. (a) Transversal homoclinic point, (b) transversal heteroclinic point.

${}_1D$, we have two invariant curves:

$$\begin{aligned} \alpha(P) = W^u(P) &= \left\{ \mathbf{u} \in \mathbf{R}^2 \mid \lim_{k \to -\infty} T^k(\mathbf{u}) = P \right\} \\ \omega(P) = W^s(P) &= \left\{ \mathbf{u} \in \mathbf{R}^2 \mid \lim_{k \to \infty} T^k(\mathbf{u}) = P \right\} \end{aligned} \tag{230}$$

We simply call $\alpha(P)$ and $\varphi(P)$ α and ω branches, respectively. We are interested in the behavior of these curves in the phase plane of T. Let P and Q be directly unstable fixed points of T. A point $\mathbf{x} \in \mathbf{R}^2$ is called a *doubly asymptotic point* if it has the asymptotic property such that

$$\alpha(\mathbf{x}) = P, \qquad \omega(\mathbf{x}) = Q \tag{231}$$

Clearly if $\mathbf{x} \in \mathbf{R}^2$ is a doubly asymptotic point, then every point in the orbit

$$Orb(\mathbf{x}) = \{\mathbf{x}_k \in \mathbf{R}^2 \mid \mathbf{x}_k = T^k(\mathbf{x}),\ k = \cdots, -1, 0, 1, \cdots\} \tag{232}$$

becomes a doubly asymptotic point. If $P = Q$, then the doubly asymptotic point is called a *homoclinic point* [see Fig. 38(a)]. Otherwise (i.e., $P \neq Q$), the doubly asymptotic point is called a *heteroclinic point* [see Fig. 38(b)]. Hence a homoclinic point approaches the saddle point P by the forward and backward iterations of T. A remarkable property found by Poincaré and developed by Birkhoff and Smale is that near a homoclinic point there exist infinitely many periodic points and a nonperiodic invariant set of T. Actually S. Smale defined the horseshoe map which exists in the neighborhood of a transversal homoclinic point as illustrated in Fig. 39. Note that a trans-

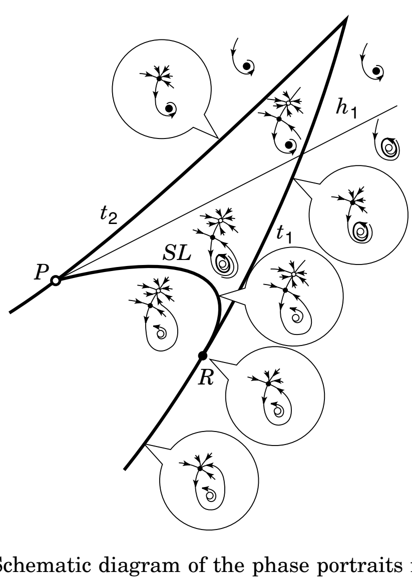

Figure 37. Schematic diagram of the phase portraits in each region or on the curve of the diagram of Fig. 36.

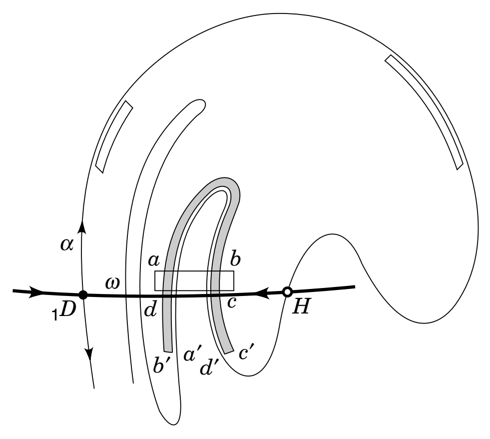

Figure 39. Schematic diagram of a horseshoe map on the small rectangle *abcd* near homoclinic points. The region comes back to the curved rectangle $a'b'c'd'$ after some finite iteration of the Poincaré map T.

versal homoclinic point is an intersection point of $\alpha({}_1D)$ and $\omega({}_1D)$ transversally—that is, not tangentially. As shown in Fig. 39, if we choose a small rectangular region *abcd* along the $\omega({}_1D)$, the image of T^k, $k = 1, 2, \ldots$, first approaches the saddle point and then leaves along the $\alpha({}_1D)$ and for some k it returns to near the original rectangular region as a curved rectangle $a'b'c'd'$ by stretching one direction and contracting the other direction. We see that the horseshoe like returned rectangle $a'b'c'd'$ intersects the original rectangle *abcd* at two parts. The map on the rectangle *abcd* is called a horseshoe map and will be discussed in next paragraph.

Example 11. Consider Duffing's equation

$$\begin{aligned} \dot{x} &= y \\ \dot{y} &= -0.02y - x^3 + 0.3\cos t - 0.08 \end{aligned} \tag{233}$$

By numerical analysis we find the phase portrait shown in Fig. 40, where the point ${}_1D$ is a directly unstable fixed point with the location $(x, y) = (-1.0278, 0.08358)$ and the multipliers $(\mu_1, \mu_2) = (0.1862, 4.7362)$. The α and ω branches intersect each other as shown in Fig. 40 and create homoclinic points. A curved rectangular region *ABCD* is mapped into the shaded region $A'B'C'D'$ by the map T. Hence T defined by Eq. (233) on *ABCD* is a horseshoe map. Note that the result is only numerically verified. Theoretically, it is very difficult to determine the behavior of these invariant curves.

Horseshoe Map

A horseshoe map on a rectangular region contains a complex invariant set. This is a typical chaotic state. Hence we summarize briefly some of the properties of the map. Let a map T have a directly unstable fixed point ${}_1D$ and let its α and ω branches intersect each other, forming homoclinic points as schematically illustrated in Fig. 41. Then the map from the rectangular region $R = ABCD$ into the plane becomes a horseshoe map. In the figure, images of the homoclinic point H_0 are

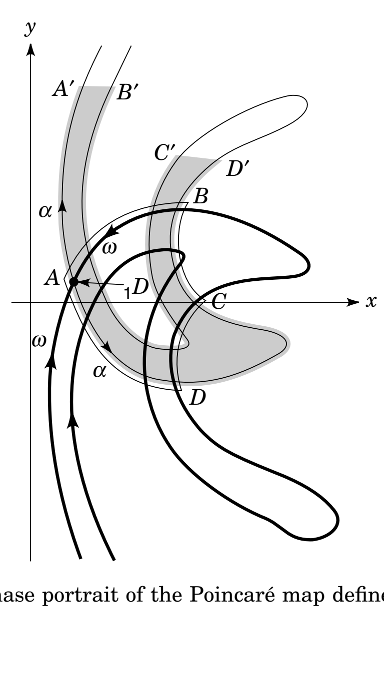

Figure 40. Phase portrait of the Poincaré map defined by Eq. (233).

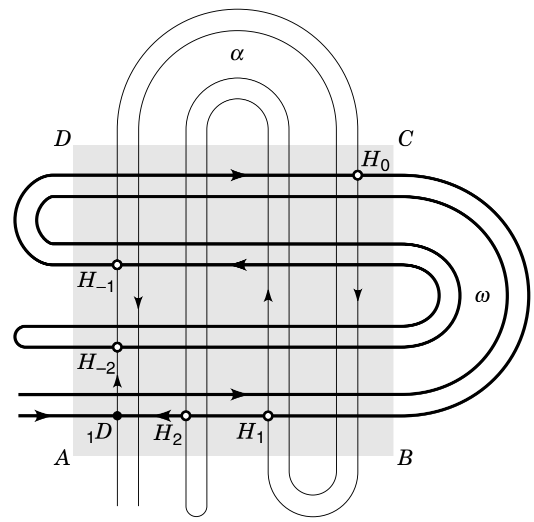

Figure 41. Schematic diagram of a horseshoe map on the rectangle *ABCD*. Invariant curves represent α and ω branches of a fixed point ${}_1D$, and a homoclinic point H_0 and its images are indicated.

indicated as

$$H_{-2} = T^{-2}(H_0), \qquad H_{-1} = T^{-1}(H_0), \qquad H_0, H_1 = T(H_0), \qquad H_2 = T^2(H_0)$$

Figure 42(a)–(c) shows the images $T(R)$, $T^2(R)$, and $T^3(R)$, respectively. We see that the number of intersections,

$$\#\{R \cap T^k(R)\} = 2^k \qquad (k = 1, 2, \ldots) \tag{234}$$

increases as 2^k while forming the vertically very narrow rectangles. And the positively invariant set becomes

$$R^\infty = R \bigcap_{k=1}^{\infty} T^k(R) \approx CantorSet \times I \tag{235}$$

Topologically, the set R^∞ has a one-to-one correspondence to the Cantor set in the horizontal direction and has an interval I in vertical direction. The same is true for the inverse iteration:

$$R_{-\infty} = R \bigcap_{k=1}^{\infty} T^{-k}(R) \approx I \times CantorSet \tag{236}$$

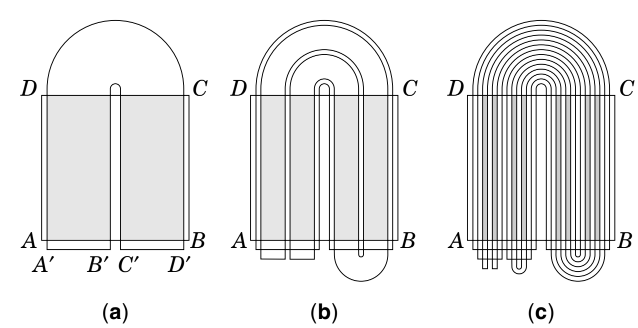

Figure 42. Schematic diagram of the images of the rectangle *ABCD* in Fig. 41 under the iteration of the Poincaré map T.

Hence the invariant set in the rectangle R has the structure

$$R_{-\infty}^{\infty} = R \bigcap_{k=1}^{\infty} T^k(R) \bigcap_{k=1}^{\infty} T^{-k}(R) \approx CantorSet \times CantorSet \tag{237}$$

By making the correspondence between the symbolic dynamics and T on $R_{-\infty}^{\infty}$, we know the following properties:

1. $R_{-\infty}^{\infty}$ has countably many periodic points of T with an arbitrarily high period, and these periodic points are all of the saddle type.
2. $R_{-\infty}^{\infty}$ has uncountably many nonperiodic point of T.
3. $R_{-\infty}^{\infty}$ has dense orbits.

Moreover, each point in $R_{-\infty}^{\infty}$ has sensitive dependence on initial conditions. That is, for any point $\mathbf{x}$ in $R_{-\infty}^{\infty}$, no matter how we choose a small neighborhood of $\mathbf{x}$, there is at least one point in the neighborhood such that after a finite number of iterations of T, $\mathbf{x}$ and the point have separated by some fixed distance. We say that T is chaotic on $R_{-\infty}^{\infty}$ or that the invariant set $R_{-\infty}^{\infty}$ is chaotic. Note that this chaotic invariant set $R_{-\infty}^{\infty}$ is unstable because of the above properties 1 and 3. To observe $R_{-\infty}^{\infty}$ as an attractor, there exists another mechanism to encapsulate this invariant set in some bounded region of the phase plane. Mathematically, this problem is not yet solved completely. In circuit dynamics, however, this mechanism may be achieved by the dissipative property of the circuit.

Example 12. Consider the phase portrait of Duffing's equation:

$$\begin{aligned}\dot{x} &= y\\ \dot{y} &= -ky - x^3 + 0.3\cos t\end{aligned} \tag{238}$$

Varying the damping coefficient k, we observe numerically the α and ω branches as shown in Fig. 43. At $k = 0.1$, we have only three fixed points: a nonresonant stable fixed point ^1S, a resonant stable fixed point ^2S, and a directly unstable fixed point D [see Fig. 43(a)]. There is no homoclinic point at this parameter. At $k = 0.05$, there appear homoclinic points, see Fig. 43(b). By decreasing k, the intersection property becomes complex as illustrated in Figs. 43(c) and 43(d).

Cascade of Period Doubling Bifurcations

One of the most popular bifurcation processes from a single fixed point attractor to chaotic state is a cascade of period-doubling bifurcations. Recall that the period-doubling bifurcation has the following bifurcational relation:

$$_0D^{2^k} \Rightarrow {}_1I^{2^k} + 2 \times {}_0D^{2^{k+1}}, \qquad k = 0, 1, 2, \ldots \tag{239}$$

In many systems with weak dissipation, this bifurcation occurs successively until k tends to infinity under the finite change of parameters. The universality of this cascade of bifurcations is studied by Feigenbaum. We illustrate this cascade by the following example.

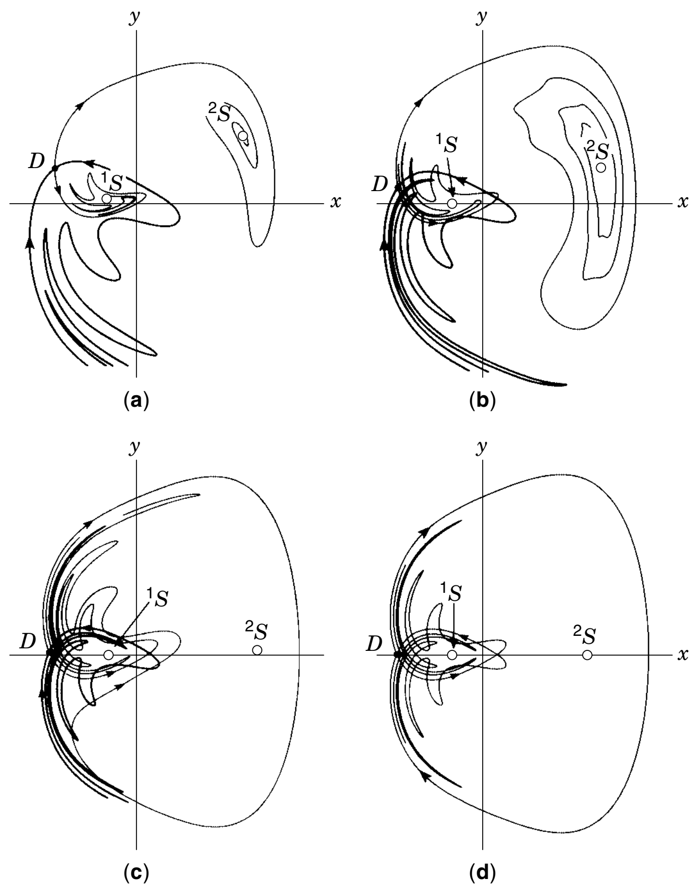

Figure 43. Phase portrait of the Poincaré map defined by Eq. (238). Homoclinic points appear when k becomes small. (a) $k = 0.1$, (b) $k = 0.05$, (c) $k = 0.005$, (d) $k = 0$.

Example 13. Consider again Duffing's equation

$$\begin{aligned}\dot{x} &= y\\ \dot{y} &= -0.1y - x^3 + B\cos t + B_0\end{aligned} \tag{240}$$

Figure 44 shows the bifurcation diagram of a fixed point corresponding to a nonresonant oscillation. P and T denote the period doubling and tangent bifurcation curves, respectively, on which these bifurcations appear. The superscript k indicates the k-periodic point, and the subscript shows the number for distinct curves. On the curve labeled $P_1^{2^k}$ the bifurcation process of Eq. (239) occurs. These curves accumulate on just the inner region of the curve P_1^8 so that in the shaded region we see a chaotic state. Phase portraits of the period-doubling cascade are shown in Fig. 45. Stable 2-periodic points exist in Fig. 45(a), which bifurcate into 4-periodic points in Fig. 45(b). Chaotic states separated into four groups appear in Fig. 45(c). They gather as two parts in Fig. 45(d) and finally coalesce into one big attractor in Fig. 45(e). The attractor grows until it touches the ω branch of the directly unstable fixed point D. After intersecting, the chaotic state loses its attractivity and the attractor disappears, although an unstable chaotic state exists.

Lyapunov Exponent to Measure a Chaotic State

To determine whether an attractor is chaotic or not, we have a conventional method of evaluating the mean value of the

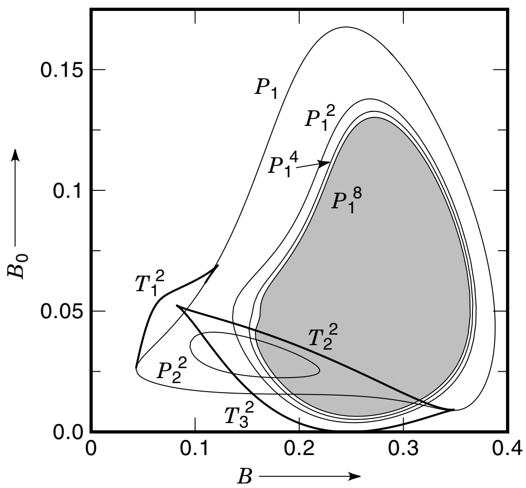

Figure 44. Bifurcation diagram of Eq. (240). Period-doubling cascade appears on a fixed point corresponding to a nonresonant periodic solution.

expansive rate of the orbit of the Poincaré map T. The mean value is known as the *Lyapunov exponent.* Consider an orbit starting from an initial point $\mathbf{x}_0 \in \mathbf{R}^2$:

$$Orb(\mathbf{x}_0) = \{\mathbf{x}_k \in \mathbf{R}^2 \mid \mathbf{x}_k = T^k(\mathbf{x}_0), k = 0, 1, 2 \ldots\} \tag{241}$$

For any vector $\mathbf{v} \in \mathbf{R}^2$ with $\|\mathbf{v}\| = 1$, the Lyapunov exponent of $\mathbf{x}_0$ with respect to $\mathbf{v}$ is defined by

$$\upsilon(\mathbf{v}, \mathbf{x}_0) = \lim_{k\to\infty} \frac{1}{2\pi k} \log \|DT^k(\mathbf{x}_0)\mathbf{v}\| \tag{242}$$

It is known that for almost all $\mathbf{v} \in \mathbf{R}^2$ with $\|\mathbf{v}\| = 1$, (a) $\upsilon(\mathbf{v}, \mathbf{x}_0) < 0$ if $\mathbf{x}_0 \in \mathbf{R}^2$ is a stable fixed point or a stable periodic point, (b) $\upsilon(\mathbf{v}, \mathbf{x}_0) = 0$ if $\mathbf{x}_0 \in \mathbf{R}^2$ belongs to a stable invariant closed curve corresponding to a stable quasi-periodic solution, and (c) $\upsilon(\mathbf{v}, \mathbf{x}_0) > 0$ if $\mathbf{x}_0 \in \mathbf{R}^2$ belongs to a chaotic attractor. Moreover, $\upsilon(\mathbf{v}, \mathbf{x}_0)$ does not depend on $\mathbf{x}_0$ and $\mathbf{v}$ in the above cases. Hence we denote simply υ and call it the maximum Lyapunov exponent. Note that Eq. (242) can be easily calculated by using the chain rule of the derivative $DT^k(\mathbf{x}_0)$ and the solutions of the variational equation with respect to the initial condition.

Example 14. As a numerical example, consider Duffing's equation in Example 13. Figure 46 shows the Lyapunov exponent. By changing parameter B we see that υ reaches zero at every period-doubling bifurcation curve and becomes a positive value at chaotic states. The discontinuous jump from the positive value to the negative value at the point marked E means the disappearance of the chaotic attractor stated in Example 13.

References in This Section

For the plane dynamical systems, many studies are reported in Refs. 32–35. The homoclinic point of the Poincaré map was studied in Refs. 36–39. Examples of Duffing's equation is found in Refs. 3 and 40. The numerical method of the computation of the Lyapunov exponent can be found in Refs. 22 and 41.

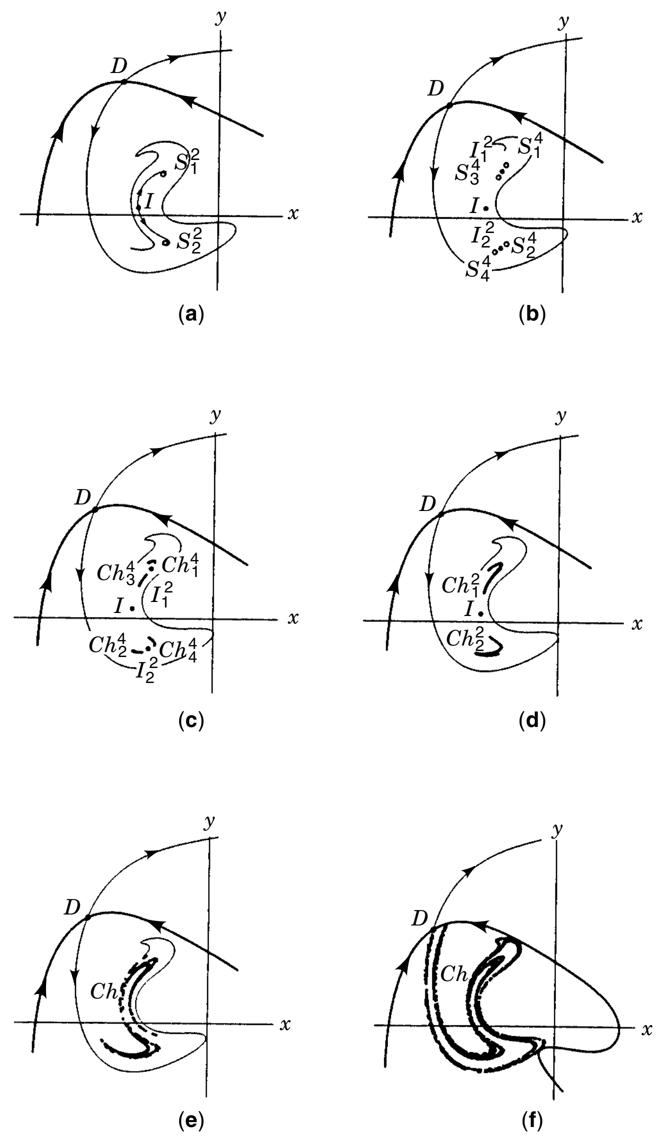

Figure 45. Phase portraits of the Poincaré map defined by Eq. (240) with $B_0 = -0.075$: (a) $B = 0.15$, (b) $B = 0.185$, (c) $B = 0.195$, (d) $B = 0.197$, (e) $B = 0.199$, (f) $B = 0.217$.

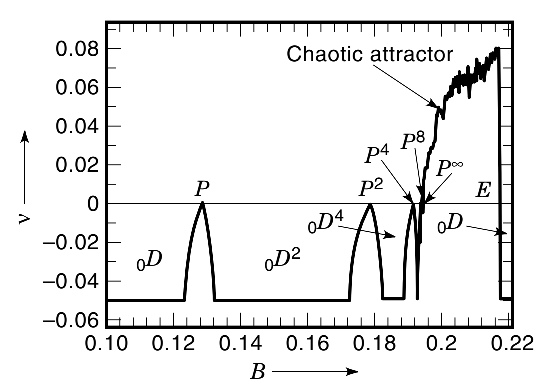

Figure 46. Lyapunov exponent of the attractors in Eq. (240) with $B_0 = -0.075$.

FURTHER REFERENCES ON NONLINEAR PHENOMENA IN CIRCUIT DYNAMICS

Thus far we have stated basic facts on nonlinear phenomena in circuit dynamics. During the last two decades, interest on nonlinear dynamics has been directed to chaotic states and related topics. Our interest is also directed to nonlinear phenomena in higher-dimensional systems. Here we briefly summarize the available books which will serve as further study on these topics.

Self-Excited Oscillations and Chaos

Simple self-excited oscillation occurs as a consequence of the Hopf bifurcation. The van der Pol oscillator stated in Examples 1(1) and 6(1) is probably the simplest sinusoidal oscillator. In higher-dimensional circuits, the same is true for this type of oscillation (see Refs. 42 and 43). As stated in the last section, we know that in two-dimensional autonomous systems, chaotic oscillation never occurs. Hence a problem arises as to how to find or design a simple chaotic oscillator. Already many circuits are proposed (see Refs. 44–47). On the other hand, how to control chaotic states is another interesting problem. Several methods are proposed for stabilizing of an unstable periodic orbit in chaotic states or, conversely, for destabilizing stable periodic state to chaotic states (see Refs. 48 and 49).

Synchronization and Chaos

Mutually coupled identical oscillators have symmetrical properties which restrict the behavior of attractors or invariant sets in state space. A group-theoretical approach has been developed for equilibria and periodic solutions (see Refs. 50 and 51). On of the interesting results is that the symmetrical property produces chaotic synchronization (see Ref. 49).

Global Bifurcations

Bifurcations in higher-dimensional systems are well summarized in Ref. 26. A zoo of bifurcation phenomena is illustrated in Refs. 7 and 52. The appearance of homoclinic and heteroclinic points produces very complicated boundary of basin of attractions, called *fractal basin boundary.* For more information on this topic, see Refs. 46, 47, 53, and 54.

BIBLIOGRAPHY

1. A. A. Andronov, A. A. Vitt, and S. E. Khaikin, *Theory of Oscillators,* Elmsford, NY: Pergamon, 1966.
2. N. N. Bogolieubov and Y. A. Mitropolskii, *Asymptotic Methods in the Theory of Nonlinear Oscillations,* New York: Gordon and Breach, 1961.
3. C. Hayashi, *Nonlinear Oscillations in Physical Systems,* New York: McGraw-Hill, 1964.
4. N. Minorsky, *Nonlinear Oscillations,* New York: Van Nostrand, 1962.
5. T. E. Stern, *Theory of Nonlinear Networks and Systems,* Reading, MA: Addison-Wesley, 1965.
6. J. J. Stoker, *Nonlinear Vibrations in Mechanical and Electrical Systems,* New York: Interscience, 1950.
7. R. Abraham and J. E. Marsden, *Foundations of Mechanics,* New York: Benjamin/Cummings, 1987.
8. V. I. Arnold, *Mathematical Methods of Classical Mechanics,* New York: Springer-Verlag, 1978.
9. J. Guckenheimer and P. Holmes, *Nonlinear Oscillations, Dynamical Systems, and Bifurcations of Vector Fields,* New York: Springer-Verlag, 1983.
10. V. I. Arnold, *Ordinary Differential Equations,* Cambridge, MA: MIT Press, 1973.
11. J. K. Hale, *Ordinary Differential Equations,* New York: Interscience, 1969.
12. M. W. Hirsch and S. Smale, *Differential Equations, Dynamical Systems, and Linear Algebra,* New York: Academic Press, 1974.
13. R. A. Rohrer, *Circuit Theory: An Introduction to the State Variable Approach,* New York: McGraw-Hill, 1971.
14. R. FitzHugh, Mathematical models of excitation and propagation in nerve, in H. P. Schwan (ed.), *Biological Engineering,* New York: McGraw-Hill, 1969.
15. M. Hasler and J. Neirynck, *Nonlinear Circuits,* Norwood, MA: Artech House, 1986.
16. L. O. Chua, C. A. Desoer, and E. S. Kuh, *Linear and Nonlinear Circuits,* New York: McGraw-Hill, 1987.
17. N. Levinson, Transformation theory of nonlinear differential equations of the second order, *Ann. Math.,* **45**: 723–737, 1944.
18. M. L. Cartwright, Forced oscillations in nonlinear systems, *Ann. Math. Stud.,* **20**: 149–241, 1950.
19. N. V. Butenin, U. I. Neimark, and N. A. Fufaev, *Introduction to the Theory of Nonlinear Oscillations* (in Russian), Moscow: Nauka, 1976.
20. K. Siraiwa, A generalization of the Levinson-Massera's equalities, *Nagoya Math. J.,* **67**: 121–138, 1977.
21. H. Kawakami, Bifurcation of periodic responses in forced dynamic nonlinear circuits: Computation of bifurcation values of the system parameters, *IEEE Trans. Circuits Syst.,* **CAS-31**: 248–260, 1984.
22. T. S. Parker and L. O. Chua, *Practical Numerical Algorithms for Chaotic Systems,* New York: Springer-Verlag, 1989.
23. E. Hairer, S. P. Norsett, and G. Wanner, *Solving Ordinary Differential Equations I and II,* New York: Springer-Verlag, 1987 and 1991.
24. I. G. Malkin, *Some Problems in the Theory of Nonlinear Oscillations,* Oak Ridge, TN: U.S. At. Energy Comm., 1959.
25. V. I. Arnold, *Geometrical Methods in the Theory of Ordinary Differential Equations,* New York: Springer-Verlag, 1983.
26. Y. A. Kuznetsov, *Elements of Applied Bifurcation Theory,* New York: Springer-Verlag, 1995.
27. H. Kawakami and T. Yoshinaga, Codimension two bifurcation and its computational algorithm, in J. Awrejcewicz (ed.), *Bifurcation and Chaos,* New York: Springer-Verlag, 1995.
28. M. Kubicek and M. Marek, *Computational Methods in Bifurcation Theory and Dissipative Structures,* New York: Springer-Verlag, 1983.
29. V. A. Yakubovich and V. M. Starzhinski, *Linear Differential Equations with Periodic Coefficients 1 and 2,* New York: Wiley, 1975.
30. N. W. McLachalan, *Theory and Application of Mathieu Functions,* New York: Dover, 1964.
31. Y. Ueda, *Some Problems in the Theory of Nonlinear Oscillations,* Osaka, Japan: Nippon Printing and Publishing Company, 1968.
32. A. A. Andronov et al., *Qualitative Theory of Second-Order Dynamic Systems,* New York: Halsted Press, 1973.
33. A. A. Andronov et al., *Theory of Bifurcations of Dynamic Systems on a Plane,* New York: Halsted Press, 1973.
34. S. Lefschetz, *Differential Equations: Geometric Theory,* New York: Interscience, 1963.

35. N. N. Bautin and E. A. Leontovich, *Methods and Examples of the Qualitative Analysis of Dynamical Systems in a Plane* (in Russian), Moscow: Nauka, 1990.

36. G. D. Birkhoff, Nouvelles recherches sur les systèmes dynamiques, *Mem. Accad. Nuovi Lincei, Ser. 3,* **1**: 85–216, 1935; also in *Collected Mathematical Papers,* New York: Dover, 1968, Vol. 2.

37. S. Smale, Diffeomorphisms with many periodic points, in *Differential and Combinatorial Topology,* Princeton, NJ: Princeton Univ. Press, 1965, pp. 63–80.

38. S. Wiggins, *Global Bifurcations and Chaos,* New York: Springer-Verlag, 1988.

39. S. Wiggins, *Introduction to Applied Nonlinear Dynamical Systems and Chaos,* New York: Springer-Verlag, 1990.

40. C. Hayashi, Y. Ueda, and H. Kawakami, Transformation theory as applied to the solutions of non-linear differential equations of the second order, *Int. J. Non-linear Mech.,* **4** (3): 235–255, 1969.

41. I. Shimada and T. Nagashima, A numerical approach to ergodic problem of dissipative dynamical systems, *Prog. Theor. Phys.,* **61** (6): 1605–1616, 1979.

42. J. E. Marsden and M. McCracken, *The Hopf Bifurcation and Its Applications,* New York: Springer-Verlag, 1976.

43. J. L. Moiola and G. Chen, *Hopf Bifurcation Analysis,* Singapore: World Scientific, 1996.

44. T. Matsumoto et al., *Bifurcations Sights, Sounds, and Mathematics,* New York: Springer-Verlag, 1993.

45. T. Kapitaniak, *Chaotic Oscillators, Theory and Applications:* Singapore: World Scientific, 1992.

46. F. C. Moon, *Chaotic and Fractal Dynamics,* New York: Wiley, 1992.

47. J. M. T. Thompson and S. R. Bishop, *Nonlinearity and Chaos in Engineering Dynamics,* New York: Wiley, 1994.

48. T. Carroll and L. Pecora, *Nonlinear Dynamics in Circuits,* Singapore: World Scientific, 1995.

49. M. Lakshmanan and K. Murali, *Chaos in Nonlinear Oscillators,* Singapore: World Scientific, 1996.

50. M. Golubitsky and D. G. Schaeffer, *Singularities and Groups in Bifurcation Theory,* New York: Springer-Verlag, 1985, Vol. 1.

51. M. Golubitsky, I. Stewart, and D. G. Schaeffer, *Singularities and Groups in Bifurcation Theory,* New York: Springer-Verlag, 1988, Vol. 2.

52. E. A. Jackson, *Perspectives on Nonlinear Dynamics,* New York: Cambridge Univ. Press, 1990, 1991, Vols. 1 and 2.

53. C. Mira, *Chaotic Dynamics,* Singapore: World Scientific, 1987.

54. C. Mira et al., *Chaotic Dynamics in Two-Dimensional Noninvertible Maps,* Singapore: World Scientific, 1996.

HIROSHI KAWAKAMI
The University of Tokushima